Thermodynamic and Biophysical Characterization of Cytochrome P450 BioI from *Bacillus subtilis*†

Rachel J. Lawson,‡ David Leys,‡ Michael J. Sutcliffe,‡ Carol A. Kemp,‡ Myles R. Cheesman,§ Susan J. Smith,⊥ John Clarkson,⊥ W. Ewen Smith,⊥ Ihtshamul Haq,|| John B. Perkins,▽ and Andrew W. Munro*,‡

Department of Biochemistry, University of Leicester, The Adrian Building, University Road, Leicester LE1 7RH, U.K., School of Chemical Sciences, University of East Anglia, Norwich, NR4 7TJ, U.K., Department of Pure & Applied Chemistry, University of Strathclyde, Thomas Graham Building, 295 Cathedral Street, Glasgow G1 1XL, U.K., Centre for Chemical Biology, Department of Chemistry, University of Sheffield, Dainton Building, Brook Hill, Sheffield, S3 7HF, U.K., and Biotechnology Research and Development, DSM Nutritional Products, P.O. Box 3255, Building 203/20A, CH-4002, Basel, Switzerland

Received April 29, 2004; Revised Manuscript Received July 23, 2004

ABSTRACT: Cytochrome P450 BioI (CYP107H1) from *Bacillus subtilis* is involved in the early stages of biotin synthesis. Previous studies have indicated that BioI can hydroxylate fatty acids and may also perform an acyl bond cleavage reaction [Green, A. J., Rivers, S. L., Cheesman, M., Reid, G. A., Quaroni, L. G., Macdonald, I. D. G., Chapman, S. K., and Munro, A. W. (2001) *J. Biol. Inorg. Chem. 6*, 523−533. Stok, J. E., and De Voss, J. J. (2000) *Arch. Biochem. Biophys. 384*, 351−360]. Here we show novel binding features of P450 BioI—specifically that it binds steroids (including testosterone and progesterone) and polycyclic azole drugs with similar affinity to that for fatty acids (K_d values in the range 0.1−160 μM). Sigmoidal binding curves for titration of BioI with azole drugs suggests a cooperative process in this case. BioI as isolated from *Escherichia coli* is in a mixed heme iron spin state. Alteration of the pH of the buffer system affects the heme iron spin-state equilibrium (higher pH increasing the low-spin content). Steroids containing a carbonyl group at the C_3 position induce a shift in heme iron spin-state equilibrium toward the low-spin form, whereas fatty acids produce a shift toward the high-spin form. Electron paramagnetic resonance (EPR) studies confirm the heme iron spin-state perturbation inferred from optical titrations with steroids and fatty acids. Potentiometric studies demonstrate that the heme iron reduction potential becomes progressively more positive as the proportion of high-spin heme iron increases (potential for low-spin BioI = −330 ± 1 mV; for BioI as purified from *E. coli* (mixed-spin) = 228 ± 2 mV; for palmitoleic acid-bound BioI = −199 ± 2 mV). Extraction of bound substrate-like molecule from purified BioI indicates palmitic acid to be bound. Differential scanning calorimetry studies indicate that the BioI protein structure is stabilized by binding of steroids and bulky azole drugs, a result confirmed by resonance Raman studies and by analysis of disruption of BioI secondary and tertiary structure by the chaotrope guanidinium chloride. Molecular modeling of the BioI structure indicates that a disulfide bond is present between Cys250 and Cys275. Calorimetry shows that structural stability of the protein was altered by addition of the reductant dithiothreitol, suggesting that the disulfide is important to integrity of BioI structure.

The cytochromes P450 are a superfamily of heme *b*-containing monooxygenase enzymes found in all major life forms (*1*, *2*). Their activity is central to synthesis and interconversions of numerous lipids, steroids and polyketides, and mammalian hepatic microsomal P450s are the front line of defense in the body against drugs and other xenobiotics (*3*). Eukaryotic P450s are, almost without exception, integral membrane proteins, and this has been a major factor hampering the determination of atomic structures for these proteins. However, genetic manipulation of microsomal CYP2C5 allowed production of a soluble monomeric form of the enzyme and enabled its crystallization and structural elucidation (*4*). Structures of other human P450s have been determined recently by industrial and academic consortia using similar strategies. By contrast, bacterial P450s are generally soluble enzymes, simplifying their expression and purification. The structures of several bacterial P450s have been solved, including forms from pathogenic bacteria (*5*) and P450s involved in catabolism of environmental pollutants (*6*, *7*) and synthesis of antibiotics (*8*).

In *Bacillus subtilis*, the genome sequence revealed eight distinct P450 systems (Table 1) (*9*). Two of these (CYP102A2 and CYP102A3) are homologues of the well-characterized *B. megaterium* enzyme flavocytochrome P450 BM3 (*10*, *11*). P450 BM3 is a fatty acid hydroxylase in which the P450 is fused to its redox partner, a flavin adenine dinucleotide (FAD)- and flavin mononucleotide (FMN)-containing cyto-

† These studies were funded by the Biotechnology and Biological Sciences Research Council (BBSRC, U.K.) and through a BBSRC studentship award to R.J.L. cofunded by DSM Nutritional Products.

* Author for correspondence: e-mail awm9@le.ac.uk; phone 0044 116 252 3464; fax 0044 116 252 3369.

‡ University of Leicester.

§ University of East Anglia.

⊥ University of Strathclyde.

|| University of Sheffield.

▽ DSM Nutritional Products.

10.1021/bi049132l CCC: $27.50
Published on Web 09/04/2004

Table 1: Cytochromes P450 and Flavocytochromes P450 Encoded in the Genome of *Bacillus subtilis*[a]

B. subtilis P450	alternative gene name(s)	genomic locus (kb)	predicted P450 M_r (Da)	closest relative (% identity)	putative role
CYP107H1	*bioI*	3089.5	44 704.8	*B. subtilis* CYP107J1 (38%)	synthesis of biotin precursor
CYP107J1	*cypA* or *yrdE*	2731.6	47 222.4	*S. erythraea* CYP107B1 (41%)	branched chain amino acid metabolism (54)
CYP134	*cypX* or *cypB*	3602.8	45 311.8	*S. coelicolor* CYP159A1 (40%)	polyketide synthesis?
CYP102A2	*cypD* or *yetO*	792.0	119 259	*B. subtilis* CYP102A3 (61%)	fatty acid hydroxylase
CYP102A3	*cypE* or *yrhJ*	2776.3	118 467	*B. subtilis* CYP102A2 (61%)	fatty acid hydroxylase
CYP152A1	*cypC* or *ybdT*	229.5	47 945.8	*Clostridium acetobutylicum* CYP152A1 ortholog (57%)	peroxide-driven fatty acid β hydroxylase
CYP107K1	*pksS*	1859.0	43 257.4	*B. subtilis* CYP107J1 (44%)	polyketide synthesis
CYP109B1	*yjiB*	1290.7	44 829.6	*B. subtilis* CYP109A1 (43%)	polyketide synthesis

[a] Cytochrome P450 systems in *Bacillus subtilis* strain 168 are listed according to their formal cytochrome P450 nomenclature (CYP number), alternative gene name, genetic locus, predicted M_r (from translated sequence), closest relative based on amino acid identity (from a BLAST search via the EBI at prohttp://ca.expasy.org/tools/blast/), and putative cellular role (based on experimental evidence or genetic context). A further P450 (CYP109) has been recognized in the distinct *Bacillus subtilis* W23 strain.

chrome P450 reductase (*12*). Another *B. subtilis* P450 is the structurally characterized P450 bsβ, which hydroxylates long-chain fatty acids at the α/β positions. Substrates for P450 bsβ are the same as those for CYP102A2 and CYP102A3, but these flavocytochromes P450 hydroxylate (as does P450 BM3) close to the ω-end of the fatty acids (*13*, *14*). P450bsβ appears not to require an accessory redox partner enzyme to deliver electrons required for reductive activation of heme iron-bound molecular oxygen. Instead it interacts directly with hydrogen peroxide, using the so-called "peroxide shunt" mechanism to facilitate oxidative catalysis (*14*, *15*). The remaining characterized *B. subtilis* P450 is P450 BioI[1] (CYP107H1), which is involved in the synthesis of biotin in this bacterium (*16*). The *bioI* gene is located at the end of an operon of genes involved in biotin synthesis, and the deleterious effects on growth induced in a *bioI* gene knockout strain confirmed involvement of the P450 in an early stage of the biotin synthesis process, leading to synthesis of pimelic acid or pimeloyl CoA (*17*). P450 BioI was reported to catalyze the oxidative cleavage of long-chain fatty acyl CoA substrates (involving multiple successive P450-mediated reactions) to produce pimeloyl CoA, a known intermediate in the biotin synthesis pathways of other bacteria (*17*, *18*). In these experiments, enzyme activity was reconstituted using a redox system involving a flavodoxin (cindoxin from *Citrobacter braakii*) as the mediator of electron transfer between a reductase and the P450 (*18*). However, other reconstituted BioI redox systems were also reported to hydroxylate fatty acids close to the ω-terminal position (*16*). In this case, activity was reconstituted using redox systems comprising *Escherichia coli* NADPH−flavodoxin/ferredoxin reductase and either *E. coli* flavodoxin or the *B. subtilis* ferredoxin (Fer) (*16*). The *B. subtilis* genome sequence revealed Fer as the only recognizable ferredoxin in the genome (*9*). Previously characterized ferredoxins in class I bacterial and eukarytotic P450 redox systems have been Fe_2S_2- or Fe_3S_4-cluster proteins (e.g., refs *19* and *20*). However, Fer is an Fe_4S_4-cluster ferredoxin that binds P450 BioI to induce heme iron spin-state perturbation and that has an appropriate reduction potential for P450 reduction (*16*, *21*).

While the capacity of BioI to bind and oxygenate fatty acids is clear and a role in synthesis of biotin appears proven, several biophysical characteristics of the enzyme remain to be elucidated. In this study, we perform a detailed structural, spectroscopic, and thermodynamic study of cytochrome P450 BioI. These studies reveal novel substrate-, steroid-, and ligand-binding features of the enzyme, the reduction potentials of the heme iron system and how they are affected by the presence of various molecules in the active site, and the likelihood that BioI contains a disulfide bond: a novel feature in a cytochrome P450 enzyme.

EXPERIMENTAL PROCEDURES

Materials. Guanidine hydrochloride (>99.0% purity) was from Invitrogen Life Technologies. Ethanol, methanol, acetonitrile, and DMSO (all 99%, anhydrous), acrylamide, and benzamidine hydrochloride were from Aldrich (Gillingham, Dorset, U.K.). Palmitoleic acid, myristic acid, and other fatty acids, testosterone and other steroids, 5,5′-dithiobis-2-nitrobenzoic acid (DTNB), and miconazole were from Sigma (Poole, U.K.). Econazole nitrate and ketoconazole were from ICN Biomedicals Inc. (Aurora, OH). Ampicillin and isopropyl-β-D-thiogalactopyranoside (IPTG) were from Melford Laboratories (Suffolk, U.K.). Yeast extract and tryptone were from Oxoid Ltd. (Hampshire, U.K.). DEAE Sepharose Fast Flow was from Amersham Biosciences (Uppsala, Sweden). Ceramic hydroxyapatite was from Bio-Rad Laboratories (Hercules, CA). Hydrochloric acid (S.G. 32%) and acetic acid were from Fisher Chemicals (Leicestershire, U.K.). Unless otherwise stated, all other reagents were purchased from Sigma and were of the highest grade available.

Expression and Purification of Cytochrome P450 BioI. Cloning and expression of BioI has been reported previously in a BL21 (DE3) pLysS host (*16*). To optimize expression and investigate influence of a putative disulfide bond, expression of BioI was analyzed in various bacteriophage T7 RNA polymerase lysogen *E. coli* strains using the pET11a expression system (*16*). These were BL21 (DE3) [F$^-$ *ompT* *hsdS*$_B$($r_b^-m_b^-$) *gal dcm* (DE3)], BL21(DE3) pLysS, BL21 *trxB* (DE3) [BL21 (DE3) *trxB*::kan], HMS173 (DE3) [F$^-$ *recA* *hsdR*($r_{K12}^-m_{K12}^+$) *Rif*^{R} (DE3)], HMS174 (DE3) pLysS; Origami B (DE3) [F$^-$ *ompT* *hsdS*$_B$($r_B^-m_B^-$) *gal dcm lacY1*

[1] Abbreviations: BioI, cytochrome P450 BioI from from *Bacillus subtilis*; DSC, differential scanning calorimetry; DTNB, 5,5′-dithiobis-(2-nitrobenzoic acid); DTT, dithiothreitol; Fer, Fe_4S_4 ferredoxin from *Bacillus subtilis*; GdmCl, guanidinium chloride; NOS, nitric oxide synthase; T_m, melting temperature.

ahpC gor522::Tn10 (Tc^R) *trxB*::kan], and AD494 (DE3) [Δ*ara-leu7697* Δ*lacX74* Δ*phoAPvuII phoR* Δ*malF3* F′ [lac^+ ($lacI^q$) *pro*] *trxB*::kan (DE3)]. All strains were from Novagen (Nottingham, U.K.). Expression was examined in small scale cultures (5 mL of Luria−Bertani (LB) medium containing appropriate antibiotics) (*22*). The strain, growth temperature, culture incubation time, and inducer (IPTG) concentration effects on BioI expression were determined by SDS−PAGE (10% acrylamide gels) of culture samples grown under different conditions. Gels were stained with Coomassie blue (0.1% Coomassie blue R-250, 40% methanol, 10% acetic acid) for 30 min at room temperature, then destained (40% methanol, 10% acetic acid) for 1 h with agitation.

Expression of BioI was carried out in Origami (DE3) using the pMG2 construct (P450 BioI in plasmid vector pET11a) described previously (*16*). Cultures (typically 6 L from 12 × 0.5 L of media in 2 L flasks) were grown in LB media using a slightly modified procedure to that described previously. IPTG induction was unnecessary for optimal enzyme production, and cultures were typically grown for 24 h from inoculation without IPTG addition. Cells were collected by centrifugation (5000*g*, 20 min, 4 °C), resuspended in 50 mM Tris·HCl containing 1 mM EDTA (buffer A) plus 1 mM benzamidine hydrochloride, and broken using a French press (three passes at 950 psi) and by sonication (Bandelin Sonoplus GM2600 sonicator on 50% full power). Extract was centrifuged at 18 000*g* (30 min, 4° C) and dialyzed twice versus 5 L of buffer A plus 1 mM benzamidine prior to loading on a DEAE Sephacel column preequilibrated in the same buffer. Protein was eluted using a linear gradient of KCl (0−500 mM) in buffer A. Fractions containing BioI were pooled and exchanged into 25 mM potassium phosphate (pH 6.5), 1 mM EDTA (buffer B) plus 1 mM benzamidine by dialysis, as before. Protein was then loaded onto a hydroxyapatite column preequilibrated in buffer B and eluted in a linear gradient of buffer B to 500 mM potassium phosphate (pH 6.5), 1 mM EDTA. BioI-containing fractions were pooled and exchanged into buffer A, as previously. Protein was further purified by ion exchange chromatography on Q-Sepharose, using the same procedure as for the DEAE step. BioI-containing fractions were concentrated by ultrafiltration and dialyzed into buffer A plus 1 mM benzamidine. A final gel filtration step was performed using Sephacryl S-200 resin. Thereafter BioI was reconcentrated by ultrafiltration to ∼1 mM, dialyzed into buffer A plus glycerol (50% v/v), and stored at −80 °C.

This treatment resulted in homogeneous enzyme as verified by spectral analysis and by SDS−PAGE analysis (10%). The enzyme concentration was determined spectrophotometrically using a difference absorption coefficient, $\epsilon_{450-490} = 91\ mM^{-1}\ cm^{-1}$, as previously described. For the fully low-spin form of BioI, this corresponds to $\epsilon_{419} = 95\ mM^{-1}\ cm^{-1}$ (*23*).

Optical Titrations. Binding of fatty acids and steroids to P450 BioI was measured by spectral titration. Fatty acid substrates induced a shift in heme iron spin-state equilibrium toward the high-spin form (type I spectral shift) concomitant with movement of the Soret peak from 417 to 394 nm. In contrast, certain steroids induced Soret spectral shifts toward the location typical of the low-spin species (reverse type I spectral shift), that is, from 394 to 419 nm. In both cases, titrations were performed by addition of small volumes of substrate or ligand (typically 0.1−0.4 μL to a total volume of ∼5 μL) across the concentration range required for saturation of the BioI active site. Spectra were recorded at each titration point. To facilitate analysis of spectral titration data, difference spectra were computed at each point in the titration. The maximal overall absorption shift induced at each point was determined by subtraction of the absorption value at the trough from that at the peak in each difference spectrum (using the same wavelengths in each case). Thereafter, values calculated in this way were plotted against the relevant ligand/substrate concentration, and data were fitted to the relevant equation. For weaker binding substrates or ligands, data were fitted to a rectangular hyperbola. For substrates or ligands with K_d values not substantially greater than the concentration of enzyme used in the assay, data were fitted instead to a quadratic function (eq 1), as described previously (*24*):

$$A_{obs} = (A_{max}/(2E_t))(S + E_t + K_d) - (((S + E_t + K_d)^2 - 4SE_t)^{0.5}) \quad (1)$$

In eq 1, A_{obs} is the absorption shift determined at the substrate or ligand concentration. A_{max} is the maximal absorption shift obtained at saturation with substrate or ligand, S, E_t is the total enzyme concentration used, and K_d is the apparent dissociation constant for the substrate− or ligand−enzyme complex.

Binding of azole drugs (ketoconazole, miconazole, econazole) was performed both using BioI in the form isolated from *E. coli* (in a mixed heme iron spin state) and with enzyme converted to low-spin state either by (a) performing titrations at pH 9.0 or (b) incubating a BioI enzyme sample (on ice) in 50 mM Tris·HCl (pH 7.2) containing 20% (v/v) ethanol for 30 min prior to exchange into alcohol-free buffer by ultrafiltration with multiple changes of buffer and reconcentration to remove the ethanol. Binding data from these experiments (Δ_{abs} versus ligand concentration) were fitted to either a rectangular hyperbola or eq 1 (for tight-binding azoles) for the titrations starting from low-spin BioI, or a sigmoidal (Hill) function (eq 2) for titrations using the mixed-spin form of BioI purified from *E. coli*, where the binding data described a sigmoid in the case of binding to certain ligands.

$$A_{obs} = A_{max}S^H/(K^H + S^H) \quad (2)$$

Molecular Modeling of the BioI Structure. To date, it has not proved possible to produce crystals of the BioI protein that diffract well enough to solve the structure of this P450. To obtain further information regarding overall structure and active site architecture of BioI and in particular to help explain our data indicating unusual molecular binding characteristics, we built a molecular model based on the known 3D structures of other P450s. Proteins of known three-dimensional structure homologous to BioI (i.e., suitable structural templates) were identified by scanning the amino acid sequence of P450 BioI against the sequences of those structures in the Protein Data Bank (*25*) using PSI-BLAST (*26*). At the time, this resulted in the P450s cam (PDB accession code 1phc (*6*)), terp (1cpt (*27*)), BM3 (2hpd (*28*)), 2C5 (1dt6 (*4*)), and eryF (1oxa (*29*)) being identified as suitable templates. These templates were used to generate comparative models by aligning them structurally to produce

a profile using Malign3D within Modeller (*30*), which was then aligned against the sequence of BioI using CLUSTALX (*31*). The resultant alignment was then checked to ensure that (i) all of the secondary structural elements have a minimum number of insertions or deletions in them and (ii) any residues crucial to catalytic activity, such as the proximal cysteinate in the fifth coordination site of the heme (*32*), were conserved. Correlation between secondary structural elements observed in a template (obtained from the Database of Secondary Structure in Proteins (*33*) [DSSP]) and the secondary structure predicted for BioI (using PSIPRED (*34*)) was used to modify the sequence alignment. Once an acceptable alignment had been produced, an ensemble of 15 models of BioI were generated using Modeller (*30*), and the "most representative" model was selected (*35*). Note that the disulfide bridge between Cys250 and Cys275 was not included as a restraint in the modeling process—it is the relative position of these two side chains in the resulting (unrestrained) model that leads us to suggest the existence of a disulfide. BioI−myristate and BioI−testosterone complexes were then modeled by docking the respective ligand into the active site using the program GOLD (*36*).

Experimental Verification of a Disulfide Bond in P450 BioI. To establish the presence of a disulfide bond in BioI, determination of solvent-accessible cysteine residues was performed using Ellman's reagent (*37*). All operations were done anaerobically (Belle Technology glovebox) unless otherwise stated. Assay buffer (100 mM potassium phosphate, pH 7.0) was deoxygenated (argon sparged) and used to prepare solutions of dithiothreitol (DTT, 50 mM) and Ellman's reagent (5,5′-dithiobis-(2-nitrobenzoic acid), DTNB, 10 mM). The product of the reaction with free thiols, 5-mercapto-2-nitro benzoate (MTNB), produces a yellow color (λ_{max} 412 nm, $\epsilon_{412} = 14\,150\ M^{-1}\ cm^{-1}$), and the formation of this product was followed over time after mixing of reagents with protein (1 h, on a Cary UV50 Bio spectrophotometer). In a control experiment, a sample of DTNB (final concentration 400 μM) in assay buffer was run as a blank, and nonspecific changes in absorption at 412 nm were monitored. In the cysteine thiol measurements on BioI, a sample of BioI (10 μM final concentration) was added to assay buffer (960 μL), and the cuvette was sealed. DTNB (40 μL, 10 mM) was injected into the cuvette, and absorbance at 412 nm was followed as above. A second duplicate sample of BioI (20 μL, 0.5 mM) was preincubated (25 °C, 1 h) with DTT (10 μL, 50 mM) in assay buffer (800 μL). DTT was then removed by gel filtration (10 DG column) in the glovebox, and the protein solution was transferred to the cuvette. The volume was made up to 960 μL, and DTNB was added as before with monitoring of ΔA_{412} for 1 h as above. Reagent-accessible thiol groups on BioI pre- and postreduction by DTT were determined using the cited extinction coefficient.

Spectroscopic Analysis: Circular Dichroism. CD spectra for BioI in the far-UV CD region (190−260 nm) were collected using a Jasco J600 spectrapolarimeter (190−260 nm) at 20 °C in a 2 mm path length cell in 50 mM Tris·HCl (pH 7.2). The sample compartments were purged with nitrogen gas to avoid absorption due to O_2. BioI protein concentration was 25 μg ml^{-1} (560 μM). Spectra were also recorded in the presence of various ligands/substrates of BioI at saturating concentrations determined from optical titrations (econazole, testosterone, and palmitoleic acid). Ligands or substrates (at minimal concentration required to saturate BioI) were delivered in DMSO (final concentration <1% v/v), and a control spectrum was recorded for BioI in the presence of DMSO alone.

Spectroscopic Analysis: Electron Paramagnetic Resonance. EPR spectra were recorded on an X-band ER-200D spectrometer (Bruker Spectrospin) fitted with a liquid helium flow cryostat (ESR-9, Oxford Instruments). The oxidized (ferric) BioI samples were prepared in Tris·HCl buffer (50 mM, pH 7.5 and 9.5) and frozen in liquid nitrogen prior to spectral acquisition. At pH 7.5, spectra were recorded for both BioI as purified from *E. coli* and the testosterone-saturated bound enzyme. A spectrum was also recorded for the purified enzyme at pH 9.5. The protein concentrations were 0.5 (ligand-bound forms) and 1.0 mM (ligand-free form), and the spectra were recorded at 10 K with microwave power = 2.01 mW and modulation amplitude = 10.0 GHz.

Spectroscopic Analysis: Resonance Raman. Resonance Raman spectra for P450 BioI were recorded using a Coherent Innova 100 krypton ion laser as the source of 413.1 nm radiation. Power at the sample was 30 mW. Scattered radiation was collected at 180°, analyzed by a Spex 1877 triple monochromator, and measured by a Princeton Instruments 1152E LN/CCD detector. Concentration of the BioI was 10 μM in 0.1 M potassium phosphate (pH 7.0). The effects of binding and ligation of various compounds upon the electronic properties of the ferric form of BioI heme were also examined using resonance Raman spectroscopy using the same BioI concentration. Ligands or substrates tested were the fatty acids myristic acid and palmitoleic acid, the steroid testosterone (all at saturating concentrations determined by optical titration studies), and the azoles 4-phenyl imidazole and econazole. Also examined was the alkaline-pH-induced low-spin form (0.1 mM potassium phosphate at pH 9.5).

Isolation and Characterization of Lipid Bound to BioI. To determine the lipid bound to the active site of BioI purified from *E. coli* (which induces a partial conversion to the high-spin form), a sample of purified BioI enzyme (1.0 μmol) was acidified (using 1 M HCl) and extracted with dichloromethane. The organic layer was dried over magnesium sulfate, and the solvent was removed under vacuum. The residue was resuspended in methanol and analyzed by electrospray mass spectrometry (mass spectra were obtained in EI mode with 70 eV ionization using a Micromass Quattro triple quadrupole mass spectrometer). To confirm identification of the sample, it was converted to a methyl ester by refluxing in acidic methanol and then analyzed by GC-MS (GC-MS analysis was performed with an RSL-150 column (25 m × 0.25 mm) on a Perkin-Elmer gas chromatograph coupled to a Micromass Quattro triple quadrupole mass spectrometer, 20 μL injection volume, ionization voltage 70 eV). The retention time, *m*/*z*, and fragmentation pattern were compared to known standards, and a library search was carried out using the instrument software.

Structural Stability Measurements: Differential Scanning Calorimetry (DSC). Differential scanning calorimetry experiments were performed to characterize heat-induced conformational transition of BioI. DSC allows determination of the unfolding transition midpoint temperature (T_m). Useful information on thermal stability of the protein in isolation

and in the presence of various ligand/substrates can be obtained. All DSC scans were performed using a MicroCal VP-DSC (MicroCal LLC, Norhampton, MA) at a heating scan rate of 1 °C/min (unless otherwise stated). The DSC was interfaced to a Gateway PIII computer and data acquisition was achieved using Origin 5.0 (MicroCal LLC, Northampton, MA). The reference cell was always filled with a buffer solution in addition to any ligand (as appropriate), and instrumental baselines were measured by placing buffer in both cells. Buffer baselines were subtracted from scans of the protein prior to data analysis using Origin 5.0 (Microcal).

A stock solution of BioI was dialyzed against 2 L of a 50 mM potassium phosphate buffer at pH 7.5 for 24 h. Dialysis buffer was stored for use in reference experiments, and the concentration of BioI was determined as stated above. A stock solution of protein (0.137 mM) was aliquoted for DSC experiments. One fraction was treated with DTT, excess DTT was removed from the enzyme by filtration through a BioRad 10DG gel filtration column in the glovebox, and the sample was sealed anaerobically immediately prior to DSC experiments. Another 1 mL fraction of the protein was scanned in the DSC without adding any DTT or ligands. In all cases, initial DSC scans were manually stopped just after T_m. The samples were then cooled back to room temperature, and the scans were repeated; this is a standard procedure for checking the reversibility of protein unfolding.

The remainder of the protein was used to investigate the effects on BioI stability of adding various substrates/ligands. These molecules were added in sufficient amounts to facilitate near-complete saturation of BioI within solubility limits of the molecules, as previously established by optical titrations. Stoichiometric concentrations of substrates or ligands were mixed with BioI: econazole, testosterone, and palmitoleic acid. DMSO solvent for these ligands or substrates was present at a constant 1% v/v in each sample. In control DSC experiments, 1% v/v DMSO was added to BioI in isolation, and the effect on enzyme stability was found to be negligible.

Structural Stability Measurements: Guanidinium Chloride-Induced Structural Perturbation. The effect of binding of substrates/ligands on the conformational stability of BioI was further examined using the chaotrope guanidinium chloride (GdmCl) and by following the perturbation of the optical spectrum of BioI (effects on chromophore environment), the aromatic amino acid fluorescence emission spectrum (environment of tryptophans), and the far-UV CD spectrum (secondary structure) in the presence of different concentrations of GdmCl.

For UV−visible analysis of BioI, enzyme (4.5 μM final concentration) was added to 50 mM Tris·HCl, 1 mM EDTA (pH 7.0) (stability buffer), followed by GdmCl in the range 0−7 M. UV−visible absorption spectra were recorded between 700 and 300 nm using a Cary UV50-Bio spectrophotometer. To monitor effects on tryptophan fluorescence, a final BioI concentration of 2 μM was used in stability buffer. For fluorescence measurements, spectra were recorded on a Varian Eclipse fluorimeter using quartz fluorescence cells of 1 cm path length. Excitation was at 290 nm with data collected between 300 and 400 nm. Excitation and emission slit widths were both set at 5 nm. For far-UV CD measurements, a final BioI concentration of 0.5 μM was used in stability buffer. For CD measurements, spectra were recorded using a Jasco J600 spectropolarimeter in the range 190−260 nm. Sample compartments were purged with nitrogen gas to avoid absorption by O_2. Effects of substrates or ligands on stability to GdmCl were analyzed by addition of near-saturating quantities to the BioI sample, as described in the Experimental Verification of a Disulfide Bond in P450 BioI section. For UV−visible, fluorescence and CD spectroscopy experiments, a stock solution of GdmCl (8 M) was prepared in stability buffer, and the appropriate volume was added to the BioI solution to give the required chaotrope concentration (0−7 M). After addition of GdmCl, the relevant BioI solution was incubated at 20 °C for 15 min prior to analysis. Data at appropriate wavelengths (reflecting maximal change in absorption, fluorescence, or CD properties) approximated sigmoids and were fitted to the Hill function (eq 2) with the parameter K^U replacing K^H used in eq 2 and reflecting the GdmCl concentration at the point at which there is 50% loss of BioI heme binding or secondary or tertiary structure.

Potentiometric Titrations. Redox titrations were performed in a Belle Technology glovebox under a nitrogen atmosphere, largely as described previously (*38*, *39*). All solutions were degassed under vacuum with argon. Oxygen levels were maintained at less than 2 ppm. The protein solutions (typically 50−100 μM in ∼5 mL of titration buffer) were titrated electrochemically according to the method of Dutton (*40*) using sodium dithionite as reductant and potassium ferricyanide as oxidant. Mediators were added to facilitate electrical communication between enzyme and electrode, prior to titration. Typically, 2 μM phenazine methosulfate, 5 μM 2-hydroxy-1,4-naphthoquinone, 0.5 μM methyl viologen, and 1 μM benzyl viologen were included (to mediate in the range between +100 to −480 mV, as described previously (*38*, *39*)). Spectra (300−800 nm) were recorded using a Cary UV-50 Bio UV-visible scanning spectrophotometer. Potentials were measured using a Pt/calomel electrode, as described previously (*38*, *39*). A factor of +244 mV was used to correct relative to the standard hydrogen electrode. Data manipulation and analysis were performed using Origin software (Microcal). Potentiometric titrations were performed for BioI enzyme purified from *E. coli* without further manipulation (i.e., in a mixed heme iron spin state), for BioI saturated with fatty acid substrate (palmitoleic acid at a final concentration sufficient to facilitate maximal extent of shift toward the BioI high-spin form, ∼100 μM), for BioI bound to the steroid testosterone (converted maximally to the low-spin complex with testosterone at ∼100 μM), and for BioI purified from *E. coli* and pretreated with ethanol (20% v/v) to remove bound lipid and convert the BioI heme to a completely low-spin form. Data for redox potential-dependent absorbance changes between 418 and 407 nm (for low-spin BioI) and between 394 and 407 nm (for high-spin BioI) were plotted against the applied potential. Data were fitted to eq 3, which represents a one-electron redox process derived by extension to the Nernst equation and the Beer−Lambert law, as described previously (*38*, *39*).

$$A = \frac{a + b10^{(E_1'-E)/59}}{1 + 10^{(E_1'-E)/59}} \quad (3)$$

In eq 3, A is the total absorbance, a and b are component absorbance values contributed by the heme in its oxidized (ferric) and reduced (ferrous) states, respectively, E is the observed potential, and E_1' is the midpoint potential for the heme iron ferric/ferrous couple. In use of eq 3 to fit the absorbance-potential data for the heme systems in the different forms of P450 BioI, the variables were unconstrained, and regression analysis provided values in close agreement to those of the initial estimates.

RESULTS

Isolation of Cytochrome P450 BioI and Identification of a Copurified Substrate. Preliminary studies focused on optimization of expression of BioI, examining a range of *E. coli* hosts strains and growth and induction conditions to determine the best conditions for production of P450 BioI from the previously reported pET11a construct (pMG2) (*16*). The Origami (DE3) strain (Novagen), which promotes cytoplasmic disulfide bond formation, was found to produce the highest levels of BioI (up to 20 mg/L of *E. coli* transformant cells), and addition of IPTG was found to be unnecessary for strong expression of BioI in most host strains. P450 was expressed without induction in Origami (DE3)/pMG2 transformant cells (typically 6 L of culture) grown in LB medium at 37 °C for 24 h following inoculation from an overnight culture. P450 BioI was purified essentially as described previously (*16*), using DEAE Sephacel, hydroxyapatite, and Q Sepharose resins. However, it was noted that the electrophoretically homogeneous enzyme so-purified exhibited a UV−visible spectrum typical of a P450 with its heme iron in a mixed spin state (i.e., with a population of both low-spin and high-spin forms), perhaps indicative of the presence of a substrate-like compound tightly bound to a large proportion of the P450 molecules. In previous studies on the P450 BSβ fatty acid peroxygenase enzyme, Shiro and co-workers established that this enzyme copurified with palmitic acid, a fatty acid abundant in the *E. coli* host (*15*).

Lipid bound to BioI was extracted using dichloromethane and subjected to electrospray mass spectrometry. This showed a predominant peak in the ES spectrum of m/z 255, giving strong indication of the presence of palmitic acid. The identity of the compound was further established by methylation and analysis by GC-MS. The retention time was identical to that for commercial palmitate methylated in house using the same protocol, and the mass spectrum of both the isolated compound and standard were similar, that is, showing the same fragmentation pattern typical of a fatty acid methyl ester. Searching a library containing examples of mass spectra of many organics and natural compounds (National Institute of Standards and Technology database) gave the identification of the isolated compound as palmitic acid. The fragmentation pattern for the sample was also the same as that for a palmitic acid standard and for that from library information, confirming palmitic acid to be the predominant compound bound by BioI in *E. coli*, as found also for P450 BSβ (*14*).

Conversion of BioI Spin-State Equilibrium by pH Change and Solvent Extraction. In light of the coisolation of palmitate with BioI purified from *E. coli*, investigations were done to establish conditions whereby the fatty acid could be dissociated from BioI and which might result in the low-spin form of the enzyme. It was found that treatment with solvents (acetonitrile or ethanol, 20% v/v) resulted in the complete conversion of BioI to a form with Soret band centered at 418 nm, indicative of the low-spin form and suggesting that the bound palmitic acid was favorably dissociated in the more apolar medium.

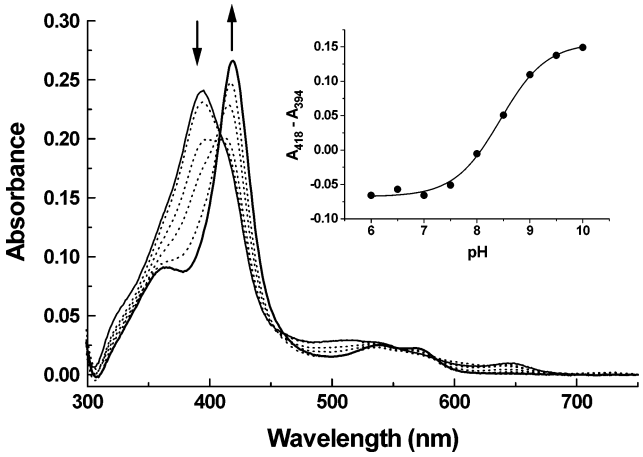

FIGURE 1: pH-dependent perturbation of optical properties of P450 BioI. UV−visible absorption spectra were recorded for fatty acid (palmitoleate)-saturated P450 BioI (2.5 μM) in the pH range between 6.0 and 10.0. Spectra shown are at pH values 6.5, 7.0, 8.0, 8.5, 9.0, and 10.0. The spectrum at pH 6.5 is shown as a thin solid line with the spectrum at pH 10.0 as a thick solid line. Spectra at intermediate pH values are shown as dashed lines. There is a progressive shift toward the low-spin form with increasing pH, indicated (with arrows) by the decreasing spectral intensity at 394 nm and increasing intensity at 418 nm. There is an isosbestic point for the spectral transition close to 408 nm. The inset shows a plot of induced absorption change in the Soret region versus the relevant pH value with data fitted to the Henderson−Hasselbalch equation for a single proton process (eq 1) in Origin software.

Through pH titrations of BioI, it was also found that increasing the pH of the buffer solution produced spectral changes indicative of an increased proportion of the low-spin form of the cytochrome (Figure 1). The effect was noted in all buffers used (sodium or potassium phosphate, Tris·HCl, or *N*-2-hydroxyethylpiperazine-*N*′-2-ethanesulfonic acid, HEPES) but was more pronounced for the organic buffers. There was an almost complete conversion to low-spin BioI by pH 9.5, and the process was freely reversible up to this pH. Using both the BioI form purified from *E. coli* and a fatty acid (palmitoleate)-saturated BioI sample, we determined the effects of pH on the proportions of low-spin and high-spin enzyme through pH dependence of optical spectra. In both cases, a plot of the extent of change to the low-spin form with pH increase produced a sigmoid, suggesting the importance of a single ionizable group, possibly reflecting the pK_a value for the interaction of the fatty acid with a protein side chain. The apparent pK_a values for the spin-state transition were 8.4 for the palmitoleate-bound enzyme and 8.4 for the (partially high-spin) form as purified from *E. coli* (Figure 1).

Binding of Substrates and Ligands to P450 BioI: Lipid Binding Studies. Binding of a number of different fatty acids was shown previously to induce shift in the heme iron spin-state equilibrium of BioI in favor of the high-spin form (*16*). This study confirms and extends this work, showing that unsaturated fatty acids, as well as long-chain saturated fatty acids, induce substrate-like high-spin shifts in the heme iron

Table 2: Dissociation Constants for Binding of Fatty Acids to P450 BioI[a]

lipid substrate	molecular formula	K_d (μM)
decanoic acid	$C_{10}H_{20}O_2$	21.5 ± 2.6
dodecanoic acid	$C_{12}H_{24}O_2$	11.0 ± 1.0
tridecanoic acid	$C_{13}H_{26}O_2$	7.7 ± 0.6
myristic acid	$C_{14}H_{28}O_2$	5.3 ± 0.5
pentadecanoic acid	$C_{15}H_{30}O_2$	5.2 ± 0.7
hexadecanoic acid	$C_{16}H_{32}O_2$	7.2 ± 0.6
octadecanoic acid	$C_{18}H_{34}O_2$	33.0 ± 5.6
myristoleic (Δ9) acid	$C_{14}H_{26}O_2$	1.5 ± 0.1
palmitoleic (Δ9) acid	$C_{16}H_{28}O_2$	0.4 ± 0.1
oleic (Δ9) acid	$C_{18}H_{30}O_2$	0.9 ± 0.1
myristoyl-CoA	$C_{35}H_{62}N_7O_{17}P_3S$	12.4 ± 0.9

[a] Binding constants were determined by optical titration of BioI at 30 °C, as described in the Experimental Procedures section. All fatty acid and fatty acid derivatives tested induced a shift in heme iron spin-state equilibrium toward the high-spin form (type I shift), as evident from a shift in Soret absorption maximum toward 394 nm.

spin-state equilibrium with absorption shifts of the heme Soret band toward 394 nm. The apparent binding constants (K_d values) for the fatty acids were determined through optical titrations, and values are shown in Table 2. Among the saturated fatty acids, the most complete shift in heme iron spin-state equilibrium is obtained with the tightest-binding C_{14} and C_{15} fatty acids myristic acid and pentadecanoic acid. However, the monounsaturated (Δ9) C_{14}, C_{16}, and C_{18} fatty acids myristoleic, palmitoleic, and oleic acid bound even more tightly to BioI than did the saturated acids, all having K_d values of <2 μM (Figure 2A). In addition the coenzyme ester myristoyl CoA was found also to bind BioI and to induce substrate-like optical shifts, albeit with affinity reduced more than 2-fold in comparison to myristic acid itself (Table 2).

In view of the apparent strong affinity for long-chain carboxylic acids, we also tested a number of similar compounds for binding to BioI to establish the importance of the carboxylate group in association with the P450 (Table 3). Because the fatty acid binding data had shown that the optimal carbon chain length for binding to BioI was 14 or 15, the compounds assessed all contained a C_{14} alkyl chain (to mimic myristic acid) with the group at C_1 being varied. The polarity of the C_1 group was altered from the nonpolar alkane tetradecane through to the highly polar amine derivative 1-amino tetradecane. This allowed us to evaluate the contribution of the C_1 group to binding of these molecules to BioI and to assess better whether the major driving force for binding of these relatively hydrophobic compounds is due to the lipophilicity of the alkyl chain and favorable interactions with the hydrophobic active site cavity of the protein, or whether ionic or hydrogen bonding interactions between the carboxylate group of the fatty acid and more polar residues (as with the interaction of fatty acid carboxylate with Arg47 and Tyr51 in the P450 BM3 system, ref *41*) play a major role in the stability of the enzyme/lipid complex.

With both the saturated and unsaturated forms of tetradecanol (1-tetradecanol and *cis*-9-tetradecen-1-ol) an initial small shift of the spin-state equilibrium of BioI toward the high-spin form was followed by a spectral conversion back to the low-spin form (A_{max} = 418 nm) at higher lipid concentrations. A possible explanation is that, at higher alcohol solvent concentrations, these molecules act as a solvent increasing the organic component of the environment

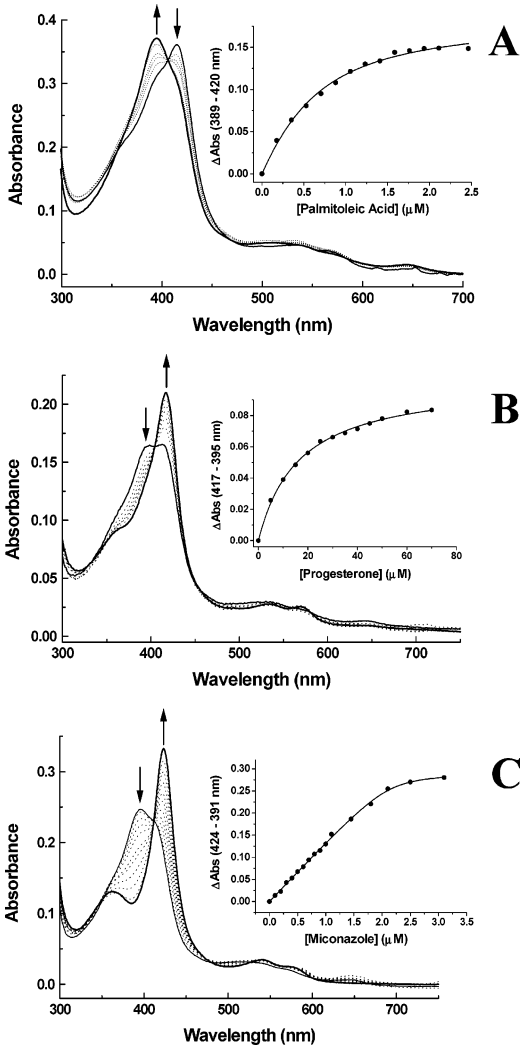

FIGURE 2: Optical spectral perturbations associated with fatty acid, steroid, and azole ligation to cytochrome P450 BioI. In panel A, binding of palmitoleic acid induces a type I (typical substrate-like) shift in the absorption features of the BioI heme with spectral maximum moving from 418 toward 394 nm (selected spectra shown). Selected spectral data are shown for titration of BioI as purified from *E. coli* (~3.6 μM, thin solid line) with palmitoleate at 0.53, 0.70, 1.23, and 1.77 μM (dotted lines). The final spectrum shown is with palmitoleate at 2.47 μM. The inset shows a fit of induced absorption shift versus palmitoleate concentration to eq 1, yielding a K_d value of 0.4 ± 0.1 μM. In panel B, binding of enone ring-type steroids induces a reverse type I-like shift in absorption features, typical of an inhibitor molecule that forces the P450 into a low-spin form with Soret band shifting to 417.5 nm. Spectral data are shown for titration of steroid-free BioI (~2.1 μM) in its starting form (thin solid line) and following addition of progesterone at 10, 15, 20, 25, and 40 μM (dotted lines). The final spectrum is for BioI following addition of 60 μM steroid (thick black line). Negligible change in spectral properties were observed after this point. The inset shows a fit of absorption shift versus the concentration of progesterone to eq 1, yielding a K_d value of 16.4 ± 0.1 μM. In panel C, binding of the polycyclic azole drug miconazole induces a shift of the Soret band to 423.5 nm on complexation with the ferric heme iron. Selected spectral data are shown for titration of BioI (~2.9 μM, starting spectrum shown as thin, solid black line) with miconazole at 0.1. 0.3, 0.4, 0.6, 0.8, 1.1, 1.45, 1.8, and 2.1 μM (dotted lines). The final spectrum is for BioI following addition of 3.2 μM azole (thick black line). Negligible change in spectral properties were observed after this point. Arrows show direction of absorption change induced on addition of miconazole. The inset shows a fit of the induced absorption shift (A_{424} minus A_{391}) versus miconazole concentration to eq 1, yielding a K_d value of 0.045 ± 0.015 μM.

Table 3: Dissociation Constants for Binding of C_{14} Alkanes, Alcohols, Alkyl Sulfates, and Alkyl Amines to P450 BioI[a]

compound name	molecular formula	shift to λ (nm)	K_d (μM)
myristic acid	$C_{14}H_{27}O_2$	394	5.3 ± 0.5
tetradecanol	$C_{14}H_{30}O$	394	0.9 ± 0.1
Δ9-tetradecanol	$C_{14}H_{28}O$	394	1.2 ± 0.2
tetradecylamine	$C_{14}H_{29}NH_2$	423	5.4 ± 0.5
tetradecyl sulfate	$C_{14}H_{29}SO_2$	393	1.0 ± 0.1
1-bromotetradecane	$C_{14}H_{29}Br$	394	1.7 ± 0.6
methyl myristate	$C_{15}H_{30}O_2$	394	3.0 ± 0.2
tetradecane	$C_{14}H_{30}$	394	0.02 ± 0.005

[a] Apparent dissociation constants for binding of tetradecanol, Δ9-tetradecanol, tetradecylamine, tetradecyl sulfate, 1-bromotetradecane, and tetradecane were determined by optical titrations at 30 °C, as described in the Experimental Procedures section. The binding constants are compared with those for the saturated C_{14} carboxylic acid myristic acid and for its methyl branched chain derivative 13-methyl myristic acid (methyl myristate). All molecules give a spectral shift indicative of promoting the high-spin form in BioI (type I shift toward 394 nm), with the exception of tetradecylamine, which gives a type II spectral shift of the Soret band to 423 nm, indicating ligation of the amine group of this molecule to the heme iron.

of the protein, withdrawing the lipids from the active site of BioI and forcing the spin-state equilibrium back toward the low-spin form. Estimates for the K_d values for 1-tetradecanol and *cis*-9-tetradecen-1-ol are calculated from a fit of the optical titration data to a rectangular hyperbola in the low lipid concentration regimes for which the C_{14} alcohols induce spectral shifts toward the high-spin form. Binding of C_{14} molecules with an electronegative group at C_1 induced a shift toward the high-spin form of BioI. 1-Bromotetradecane, 1-tetradecyl sulfate, and methyl myristate bound tightly to BioI (K_d values <3.0 μM) but induced a less-complete conversion toward the high-spin form than did saturating levels of myristic acid. In the case of methyl myristate, the conversion to the high-spin form at saturation was at least 80% of that with myristic acid, but in the case of 1-bromotetradecane and 1-tetradecyl sulfate, the proportionate changes were ~60% and ~30%, respectively. Tetradecylamine gave an inhibitory shift due to the presence of the sp^3 nitrogen, which ligates the heme iron, as indicated by a shift in the Soret band to 423 nm (a type II shift, as observed with interaction of the heme iron with the sp^2 hybridized nitrogens of imidazole). The tight binding of tetradecylamine is clearly facilitated by its C_{14} alkyl chain, as is also seen with the fatty acid-linked imidazole derivatives (K_d values < 3.0 μM, cf. imidazole with a $K_d > 200$ μM). These findings suggest that the relative contribution of the carboxylate to the binding energy of fatty acids is considerably less than that provided by interactions between the alkyl chain and the BioI binding pocket. This is further confirmed by analysis of the binding data for the less water-soluble tetradecane. While this compound did induce a shift in the heme iron spin-state equilibrium toward high-spin (despite the absence of an electronegative group on its α carbon), near-complete conversion of BioI to the high-spin form was not obtained with residual absorption indicative of the low-spin component remaining at the end point in the titration. Saturation with tetradecane produced ~30% of the conversion to the high-spin form observed at the endpoint of the titration with myristic acid itself. Thus, the binding of tetradecane illustrates that the balance between compound solubility in aqueous media and the complementarity between the substrate and the active site cavity are of as much importance as the presence of an electronegative group on the substrate as regards efficiency of spin-state conversion of the P450 heme iron.

Binding of Substrates and Ligands to P450 BioI: Binding of Steroids to P450 BioI. The genome sequence of *B. subtilis* revealed the presence of eight putative cytochrome P450 enzymes, of which BioI and at least three others have been shown to bind fatty acids (Table 1, *42*). The other three enzymes are the flavocytochromes P450 102A2 and 102A3 (homologues of the well-characterized P450 BM3 enzyme, *13*) and the peroxide-driven fatty acid hydroxylase P450 BSβ (*13*, *43*). Amino acid sequence alignments with the P450 BSβ and the heme domains of the two flavocytochrome P450s revealed rather low levels of identity between these *B. subtilis* fatty acid-binding P450s and BioI (22.3% identity with heme domain of flavocytochrome P450 102A3 over the 395 amino acids of BioI, 18.7% with P450 102A2, and 20% with P450 BSβ). However rather higher levels of amino acid sequence identity were found with three of the other *B. subtilis* P450s, none of which have been characterized as fatty acid metabolizing enzymes (38.7% identity with CYP107J1, 35.7% identity with CYP107K1, and 30.9% identity with the putative P450 product of the *B. subtilis yjiB* gene). Among these, CYP107K1 is a potential hydroxylase of polyketides synthesized by the *pks* gene products of *B. subtilis*. In addition, BioI showed higher levels of identity with several actininomycete P450s, many of which may also be involved in metabolism of polyketides, polycyclics or both. Among the structurally characterized P450 isoforms, BioI shows strongest sequence identity with P450 eryF (CYP107A1) from *Saccharopolyspora erythraea*, a P450 involved in hydroxylation of the polyketide 6-deoxyerythronolide B (34.2% identity, 70.4% similarity over the full length of BioI). P450 eryF has been shown to bind tightly to steroids and polycyclic aromatic hydrocarbons (*44*).

In view of the apparent closer identities with P450s involved in metabolism of polycyclics, we tested a variety of sterol, steroid, polyketide, and polycyclic compounds for binding to BioI, using spectral perturbation as a marker for molecular interactions in the active site. Spectral changes were observed with the steroid molecules androstenedione, hydrocortisone, testosterone, corticosterone, progesterone, and 6α-methyl-17α-hydroxy-progesterone acetate but not with the steroid and steroid-like molecules 3-[(3-cholamidopropyl)dimethylammonia]-1-propanesulfonate (CHAPS), cholesterol, estrone, β-estradiol, 5-pregnen-3β-ol-20-one, and prednisolone. An obvious difference between those steroid molecules that did or did not give rise to spectral changes is the presence of a carbonyl group on the 3-position of the A-ring (i.e., a conjugated carbonyl rather than a phenol ring, Figure 3). The nature of the spectral shift observed was an apparent reverse type I shift, whereby there is spectral conversion to a species similar to that observed for the completely low-spin form of BioI (i.e., with Soret maximum at 419 nm). However, at this stage it remained unclear as to whether this type of spectral shift arose indirectly from an effect of spin state induced by binding of steroid in the vicinity of the heme or through direct coordination of the steroid carbonyl group as the distal axial ligand to the heme iron. Optical binding titrations were performed with androstenedione, hydrocortisone, testosterone, corticosterone, proges-

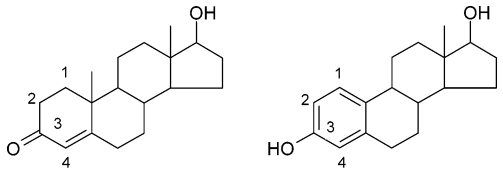

FIGURE 3: Influence of steroid structure on P450 BioI interactions. Molecular structures of the steroid hormomes testosterone (A) and β-estradiol (B) are shown. Steroids, such as testosterone, containing the enone type A ring (numbered with carbonyl at C_3), bind tightly to BioI, inducing spectral conversion. By contrast, no spectral changes are induced by steroids containing the phenol A ring. Apparent K_d values for enone-type steroids are affected by substituents on the D ring, but binding per se is not prevented.

Table 4: Dissociation Constants for Binding of Steroids to P450 BioI[a]

steroid	K_d (μM)
andostenedione	133 ± 5
hydrocortisone	62.8 ± 6.1
progesterone	16.4 ± 0.7
testosterone	6.6 ± 0.3
corticosterone	157 ± 14
6α-methyl-17α-hydroxy-progesterone acetate	139 ± 21

[a] Dissociation constants for binding of steroids with carbonyl group at the 3-position on the "A" ring (see Figure 3) were determined by optical titration at 30 °C, as described in the Experimental Procedures section. These steroids induced a type II (or reverse type I) P450 spectral change with a shift in Soret absorption maximum toward 418 nm.

terone, and 6α-methyl-17α-hydroxy-progesterone acetate, using an extensively high-spin (palmitate-bound) preparation of BioI in each case (Figure 2B). From these titrations, apparent binding constants for these steroids were determined (Table 4). The failure of other steroid and steroid-like molecules to induce any significant spectral shift with the same extensively high-spin preparation of BioI suggested that these molecules had minimal affinity for the BioI active site within their range of solubility. In the case of those molecules with the aromatic "A" ring, this is likely to be a consequence of the nonplanarity of the steroids at this part of the structure. In parallel studies, no spectral perturbations were detected on addition of the polyketides tylosin tartrate or erythromycin or the polycyclic aromatic hydrocarbons phenanthrene, 9-amino phenanthrene, and fluorene.

Binding of Substrates and Ligands to P450 BioI: Azole Drug Binding. In view of the apparent diversity in molecular structures found to bind P450 BioI, binding of various commercially available azole-based inhibitors was done to probe further the spatial properties of the BioI active site and the effects of aromatic and alkyl substitutions on affinity for azole derivatives. Binding of all azoles induced a type II shift in the heme spectrum, the Soret band shifting to a maximum at longer wavelength (between 423 and 425 nm). As above, K_d values were determined from optical titrations with the azole drugs (Table 5). The binding of imidazole itself was relatively weak ($K_d = 208 \pm 15$ μM), as was that for 4-bromo-1*H*-imidazole ($K_d = 348 \pm 20$ μM). 4-Phenylimidazole, a compound used successfully in crystallization of P450s, bound somewhat more tightly ($K_d = 16.5 \pm 0.55$ μM). However, attachment of an alkyl chain ($C_{10}-C_{12}$) to the imidazole resulted in a >100-fold improvement in binding for these molecules, as might be expected for a fatty acid-binding enzyme. Remarkably, the K_d values for the binding of the polycyclic azole drugs econazole, miconazole, and ketoconazole was also extremely tight. These data indicate that the active site of BioI is relatively large and flexible and can accommodate favorably both long alkyl chain-containing molecules and polycyclics.

Table 5: Dissociation Constants for Binding of Azole Inhibitors to P450 BioI[a]

azole inhibitor	molecular formula	K_d (μM)
imidazole	$C_3H_4N_2$	208 ± 15
Im-C10	$C_{13}H_{23}N_2O_2$	2.6 ± 0.2
Im-C11	$C_{14}H_{25}N_2O_2$	1.5 ± 0.2
Im-C12	$C_{15}H_{27}N_2O_2$	1.0 ± 0.2
4-bromo-1*H*-imidazole	$C_3H_3N_2Br$	348 ± 20
4-phenylimidazole	$C_9H_8N_2$	16.5 ± 0.6
econazole[b]	$C_{18}H_{15}Cl_3N_2O$	0.37 ± 0.01 (0.016 ± 0.009)
miconazole	$C_{18}H_{14}Cl_4N_2O$	2.01 ± 0.35 (0.045 ± 0.015)
ketoconazole[b]	$C_{26}H_{28}Cl_2N_4O_4$	2.31 ± 0.35 (0.034 ± 0.008)

[a] Dissociation constants for binding of a number of azole-based inhibitors to P450 BioI were determined by optical titrations at 30 °C at pH 7.0, as described in the Experimental Procedures section. The azoles used included the ω-imidazolyl carboxylic acid derivatives of lauric acid (ImC12), undecanoic acid (ImC11) and decanoic acid (ImC10) (*53*) and the azole antifungal drugs econazole, miconazole, and ketoconazole. Binding constants were determined by fitting absorption shift versus azole concentration data to a rectangular hyperbola or (where K_d values were <10 μM) to eq 1 describing tight-binding ligands. Values in parentheses for the binding of the azole antifungal drugs are from titrations performed at pH 9.5. In these cases, all azoles bound much tighter than at pH 7.0, and data were fitted to eq 1. [b] In the case of the binding of econazole and ketoconazole to BioI at pH 7.0, the binding plots were distinctly sigmoidal and were fitted best to eq 2 to derive the apparent K_d values.

While binding of imidazole, the small substituted imidazoles, and the imidazolyl carboxylic acids gave rise to "normal" hyperbolic plots of induced absorption change versus ligand concentration, the azole antifungal drugs econazole and ketoconazole produced sigmoidal binding curves with BioI that fitted best to eq 2. Miconazole bound to BioI rather more tightly, and in this case, the data fitted best to eq 1 (Figure 2C). This apparent cooperative binding of ligand has been observed previously in studies of P450s, including recent studies of P450 eryF. In the case of the androstenedione- and 9-aminophenanthrene-bound structures of P450 eryF, two molecules of these ligands are present in the active site, indicating that there may be true homotropic cooperativity in binding. In the case of BioI, earlier studies had shown that palmitic acid copurified with the enzyme. Thus, the possibility existed that residual amounts of this molecule were responsible for the unusual binding phenomenon. In view of this, azole antifungal binding titrations with BioI were repeated at pH 9.5, under which conditions the BioI spectrum indicates that the heme iron is almost completely low-spin. Under these conditions, the form of the binding curve was clearly hyperbolic for each of the three azole antifungal drugs tested, suggesting that apparent cooperativity observed at pH 7.0 could be due to interactions between palmitate and the azole antifungals and that on weakening of fatty acid binding at high pH these azole drugs exhibit normal single site reversible binding properties. In addition, all of the azole antifungal drugs bound considerably more tightly at the higher pH, suggesting that palmitate probably obstructs the binding of these azoles (Table 5).

Alkaline pH did not lead to spectral shifts for the testosterone-bound enzyme, indicating that the steroid remained bound tightly, possibly facilitated by a steroid carbonyl−heme iron interaction. In parallel studies, it was found that "extraction" of the endogenously bound fatty acid could be achieved by brief mixing with solvent (up to 20% v/v acetonitrile or ethanol), resulting in conversion of the enzyme to a low-spin form. Binding of azole antifungal drugs to the solvent-treated BioI (following gel filtration to remove the solvent) again resulted in hyperbolic ligand-binding plots, as observed for the pH 9.5 titrations.

Molecular Modeling of the BioI Structure. Work to crystallize the BioI protein has to date failed to produce crystals that diffract well enough to solve the structure of the P450. To obtain further information regarding the overall structure and active site architecture of BioI (in light of above binding data indicating unusual molecular binding characteristics), we built a molecular model based on structures of existing homologous P450 enzymes (see Experimental Procedures section). The model suggests that the active site of BioI is predominantly hydrophobic in nature, in common with other P450s. Residues lining the active site include Phe83, Leu84, Ala235, (the side chain methyl of) Thr239, and Phe384. Two particularly interesting points about BioI−ligand interactions are suggested by the model.

First, myristate is predicted to bind with the ω end of the molecule close to the heme (as is seen for P450 BM3, *45*). This suggests that BioI could catalyze hydroxylation close to the ω-terminus. However, this model appears to rule out the possibility of oxidation of the C_{14} fatty acid at central carbon atoms. In a previous study of BioI, sequential oxidative attack of fatty acid bound to ACP protein copurified with BioI or of palmitic acid was reported to produce very small amounts of the C_7 dicarboxylic acid pimelate (*18*). This was postulated to occur through three consecutive BioI-catalyzed oxidative reactions at the ω-9 carbon (in the case of palmitic acid, ω-7 for myristic acid). A distinct result suggesting hydroxylation close to the ω-terminus was obtained by Green et al. (*16*). In more recent work, Cryle et al. confirm that BioI-mediated hydroxylation occurs near the ω-position (at ω-1, ω-2, and ω-3 for myristic acid), albeit in a system with a large (15-fold) excess of enzyme over substrate (*46*). The modeling data with myristic acid favors strongly the hydroxylation of fatty acids close to the ω-terminus due to a constriction in the size of the active site close to the ω-2 position that would occlude the extra bulk required for successive oxidative reactions around the ω-7 carbon. The model also predicts that the carboxyl group of myristate may hydrogen bond with the side chain hydroxyls of Ser67 and Thr179.

Second, testosterone is predicted to bind with the C_3 carbonyl close to, and potentially interacting with, the heme iron, consistent with experimental results that suggest that the steroid carbonyl group may interact with the heme iron. The modeling studies suggest that the alternative orientation with the C_{17} hydroxyl and C_3 carbonyl juxtaposing positions does not occur due to the position of Glu65. This is predicted to be a hydrogen bond acceptor for the C_{17} hydroxyl but is not able to form an equivalent interaction with the C_3 carbonyl.

A further major feature evident from modeling of the BioI structure is that the side chains of two cysteine residues

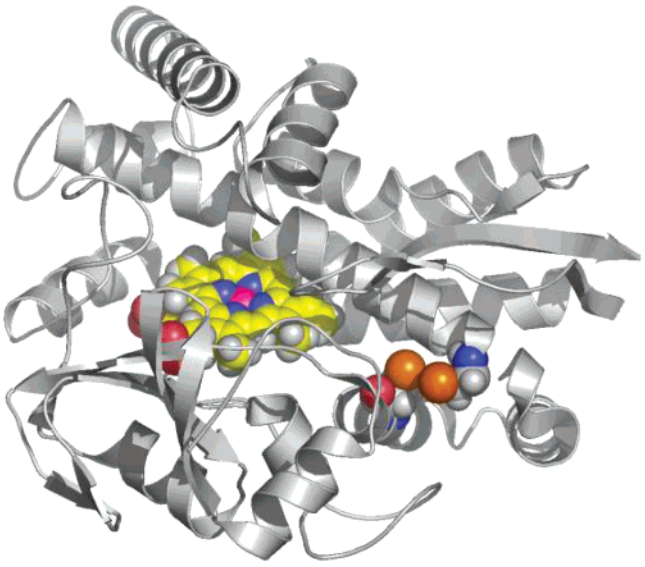

FIGURE 4: Molecular model of P450 BioI. A model structure for cytochrome P450 BioI was generated as described in the Experimental Procedures section. Secondary structural features (helices and sheets) are depicted in gray. The heme is shown in yellow space-fill with the heme iron in red and equatorial coordinating nitrogens in blue space-fill. A disulfide bridge predicted between Cys250 and Cys275 is indicated with the bonded sulfur atoms shown in orange space-fill. Cys275 is to the right, located near one of the termini of the long I helix in P450 BioI.

(Cys250 and Cys275) are located in close proximity to one another (separated by 4.1 Å). This suggests that a disulfide bond between these amino acids may be present on the surface of the protein. The putative disulfide is located 11.1 Å from the heme macrocycle at the closest point from the disulfide bridge heme (Figure 4). No structural evidence exists to date for the presence of disulfide bonds in any other cytochrome P450 enzyme.

Verification of a Disulfide Bond in BioI. Modeling data for the BioI structure suggest strongly the presence of a disulfide bond between Cys250 and Cys275, predicting that the side chains of these residues approach within 4 Å. In addition, expression of BioI was found to be optimal in the *E. coli* strain Origami B (DE3), which has *gor*/*trxB* mutations, promoting disulfide bond formation (Novagen), consistent with the proposal that a disulfide bond is present in BioI and that this affects the stability of the expressed enzyme. To confirm the presence of a disulfide bond, we determined the number of free thiols in P450 BioI using Ellman's reagent, both in the oxidized enzyme form and following anaerobic reduction of BioI with dithiothreitol (DTT) to reductively cleave any disulfide bridges (*37*). When the same preparation of enzyme was used for both anaerobic assays, the number of free cysteine thiols was 0.5 ± 0.1 for the fully oxidized enzyme, rising to 2.0 ± 0.2 for the DTT-reduced form. These data indicate the exposure of additional cysteines on DTT addition, consistent with the disruption of a disulfide bond between Cys250 and Cys275 in the P450. To our knowledge, this is the first example of a disulfide bond in a cytochrome P450 enzyme.

Analysis of the Structural Stability of P450 BioI: Electronic Spectroscopy. Guanidinium chloride (GdmCl)-induced disruption of heme ligation and subsequent loss of the heme cofactor from BioI (in various substrate- or ligand-bound forms) was followed by electronic absorption spectroscopy.

All BioI forms underwent similar spectral changes as GdmCl concentration was elevated with decreases in Soret intensity and a shift in spectral maximum toward ~370 nm at high GdmCl concentration. The loss of intensity and spectral shift is correlated with dissociation of heme from its cysteinate-ligated state and ultimately from the protein matrix. Plots of the extent of conversion of the spectral species against GdmCl concentration in the range 0−7 M were sigmoidal, and fits of these data to the Hill function (eq 2) produced estimates for the midpoint concentration of GdmCl required to dissociate 50% of the heme from its native form. These midpoint K^U values were very similar for the palmitate-bound form purified from *E. coli* (mixed-spin), low-spin and low-spin DTT-treated, and steroid-bound (testosterone, progesterone) BioI. In all cases, the K^U value was in the range of 2.5 ± 0.3 M. Heme binding in the low-spin form at pH 9.5 was considerably weakened with a K^U of 1.5 ± 0.2 M GdmCl. However, in various ligand-bound forms (econazole, 4-phenylimidazole), the midpoint is much higher at 3.6 ± 0.2 M, suggesting stabilization of heme binding by the presence of the azole ligands to the heme iron (Figure 5A). These data are consistent with resonance Raman studies of the azole complexes of BioI, where tighter heme binding is inferred (see below).

Analysis of the Structural Stability of P450 BioI: Fluorescence Spectroscopy. Fluorescence from tryptophan residues was measured as a function of GdmCl concentration to establish whether stability of tertiary structure was affected according to the substrate- or ligand-bound status of BioI. Modeling of the structure of BioI predicts that the three trytophan residues (Trp37, Trp161, and Trp376) may all be at least partially solvent-exposed on the protein surface. Thus, a large increase in tryptophan fluorescence on unfolding of BioI was not expected. This is seen to be the case with the fluorescence emission intensity from the native BioI protein at 0 M GdmCl (regardless of presence of substrate or ligand) being similar to that observed for fully unfolded enzyme at 8 M GdmCl. The emission wavelength maximum is at 340 nm for native BioI, shifting to 358 nm for the unfolded form. There is a progressive shift in emission maximum wavelength at intermediate GdmCl concentration, reflecting the equilibrium between various states. At intermediate concentrations of GdmCl, the fluorescence intensity decreases to a minimum at ~2.5 M GdmCl with fluorescence intensity around 50% of that for the starting form, prior to rising again as the fully unfolded state is approached (Figure 5A).

To determine the midpoint GdmCl concentration for tertiary structure loss through analysis of change in tryptophan fluorescence, ratios of fluorescence at the wavelength maxima for fully folded (340 nm) and fully unfolded (358 nm) forms were plotted against GdmCl concentration, and data were fitted to a sigmoidal function (eq 2). The midpoint for the ligand-free BioI was 1.55 ± 0.15 M GdmCl, within error of that determined in the presence of DTT (1.62 ± 0.15 M). The tertiary structure stability was diminished at pH 9.5 (1.29 ± 0.22 M), possibly reflecting destabilization of BioI by alteration of protonation states of key residues involved in stability or through increased nucleophilicity of the guanidinium ion. Addition of substrates (palmitoleate 2.1 ± 0.1 M; myristate 2.4 ± 0.2 M), steroids (progesterone 2.6 ± 0.2 M) and ligands (econazole 2.3 ± 0.2 M) had some stabilizing effects (Figure 5B).

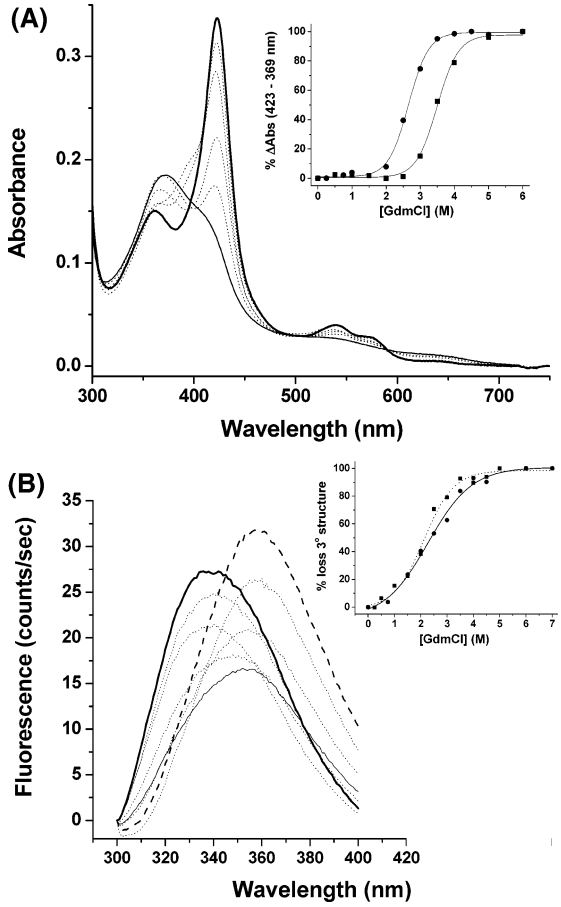

FIGURE 5: Structural stability of P450 BioI to denaturation by guanidinium chloride. In panel A, the main figure shows the optical properties of the 4-phenyl imidazole-bound P450 BioI (3.5 μM) in the absence of denaturant (thick solid line). Subsequent spectra in dotted lines (at 0.5, 1.5, 3.5, 4, and 6 M GdmCl) show the progressive diminution of the native-like Soret feature at approximately 423 nm with the development of a smaller absorption feature at approximately 369 nm, reflecting heme dissociated from cysteinate ligation. The final spectrum at 6 M GdmCl is shown as a thin solid line. The inset shows an overlay of the ΔA data (A_{423} minus A_{369}) for the 4-phenyl imidazole-bound (■) and palmitoleic acid-bound (●) forms of P450 BioI. Data are fitted to a sigmoidal function (eq 2), producing midpoint values of heme dissociation of 2.7 ± 0.1 M for the palmitoleic acid-bound form and 3.5 ± 0.1 M for the 4-phenyl imidazole-bound form. In panel B, the main figure shows the aromatic amino acid fluorescence emission spectra collected from the econazole-bound form of P450 BioI (2 μM) in the absence of the chaotrope GdmCl (thick, solid black line) and in the presence of 0.5, 0.75, and 1.5 M GdmCl (dotted lines, decreasing fluorescence at 340 nm), 2.5 M GdmCl (thin, solid line), 3 and 5 M GdmCl (dotted lines, increasing fluorescence at 358 nm), and 6 M GdmCl (thick, dashed line). The inset shows an overlay of the maximal changes in fluorescence (expressed as a normalized ratio of the fluorescence values at 358 and 340 nm and presented as a proportion of overall change in the tertiary structure of the protein) for the econazole- (●) and palmitoleic acid-bound (■) forms of BioI. The data are fitted to a sigmoidal function (eq 2), producing midpoint values of BioI tertiary structure loss of 2.3 ± 0.1 M GdmCl (econazole-bound) and 2.1 ± 0.1 M GdmCl (palmitoleic acid-bound).

Analysis of the Structural Stability of P450 BioI: Differential Scanning Calorimetry. Differential scanning calorimetric studies of BioI were performed with the enzyme in its native form and in complex with testosterone, econazole, and palmitoleate. Analysis of the effects of pretreatment with DTT was also undertaken using DSC to establish whether there were measurable effects on thermal stability induced

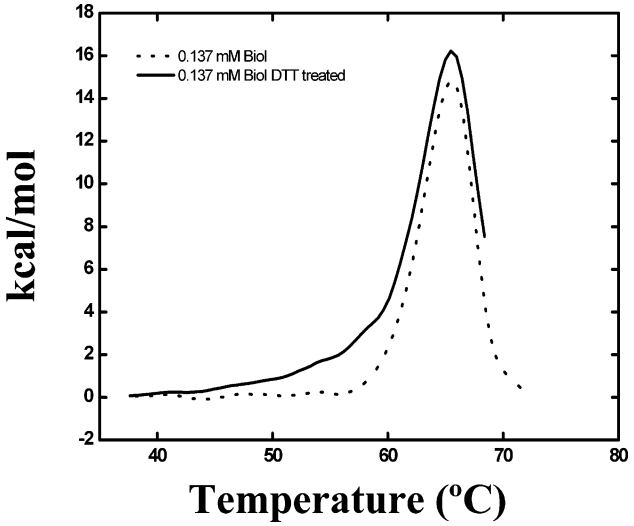

FIGURE 6: DSC analysis of P450 BioI. DSC scans are shown for BioI (137 μM) in the presence (—) and absence (···) of DTT. Excess DTT was removed from the sample as described in the Experimental Procedures section. A buffer baseline has been subtracted from the raw data, and the scans have been normalized for molar concentration and scan rate. In both cases above, the protein unfolds irreversibly; however, the T_m for the transitions, both with and without DTT, is 65.5 °C.

by reductive cleavage of the disulfide. Figure 6 shows the results of DSC scans conducted with the form of BioI isolated from *E. coli* in the presence and absence of DTT. These studies reveal that in all cases BioI melts irreversibly and, therefore, analysis based on equilibrium thermodynamics cannot be used to extract thermodynamic parameters from the data. However, it is possible to use the transition midpoint (i.e., T_m) to quantify protein stability. In this case, the protein has a T_m of 65.5 °C, and it is not affected by the presence of the reducing agent DTT. Closer examination of Figure 6 shows that BioI unfolding in the presence of DTT may be more complex than in the absence of reducing agent. There is clear evidence of a small shoulder in the DSC endotherm in the temperature range 50−60 °C. Therefore melting is clearly non-two-state in the DTT-reduced form, as it appears to be in the absence of DTT.

DSC analysis of the various substrate- and ligand-bound forms of BioI revealed again that, in all cases, a single melting temperature (T_m) was observed with irreversible endotherms and protein aggregation at temperatures above the T_m. The values for T_m in the presence and absence of ligands (after scan rate normalization), as well as ΔT_m values (with respect to substrate-free protein), are collated in Table 6. There is an apparent destabilization of BioI by fatty acid with the palmitoleate-bound enzyme having a T_m 4.3 °C lower than that for the substrate-free enzyme. The effect on protein stability of the steroid testosterone is negligible, and econazole, at best, only induces a very modest stabilization.

Spectroscopic Analysis. Spectroscopic characterization of P450 BioI was undertaken using circular dichroism, resonance Raman, and EPR to define further the structural properties of the enzyme and examine in detail the features of its heme center. The far-UV CD spectrum of BioI is typical of a helix-rich protein (as expected for a P450) and resembles closely the far-UV CD spectrum of the heme domain of the structurally characterized P450 BM3 enzyme (*47*). BioI has CD spectral minima at ~209.5 and 218.5 nm

Table 6: Calorimetrically Derived T_m Values for the Unfolding of BioI in the Presence and Absence of Substrates or Ligands[a]

substrate or ligand	T_m (°C)	ΔT_m (°C)
free BioI	65.5	
econazole	66.2	+0.7
palmitoleate	61.2	−4.3
testosterone	65.6	+0.1

[a] DSC was performed as described in the Experimental Procedures section. The T_m for unfolding of BioI in the presence and absence of DTT was 65.5 °C. Binding of the azole drug econazole and the steroid testosterone had minor effects on the T_m, but there was an apparent destabilization (ΔT_m) of 4.3 °C in the presence of the tight-binding fatty acid substrate palmitoleate.

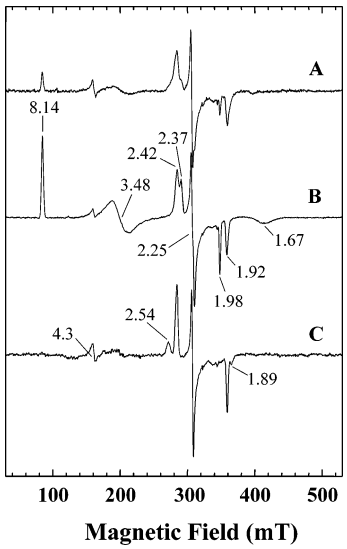

FIGURE 7: EPR spectra for P450 BioI. EPR spectra are shown for P450 BioI in the testosterone-bound form (panel A, extensively low-spin) and in the forms isolated from the *E. coli* expression host and recorded at pH 7.5 (panel B, mixed-spin state) and pH 9.5 (panel C, extensively high-spin). Relevant *g*-values for the major low-spin form are at 2.41, (g_z), 2.25 (g_y), and 1.92 (g_x) and for the high-spin form at 8.14, (g_z), 3.14 (g_y), and 1.67 (g_x). Spectra were recorded as described in the Experimental Procedures section.

and a crossover point at 201 nm. The effects of addition of various substrates and ligands to the spectrum were determined. The effects of the denaturant guanidinium chloride (GdmCl) on the stability of BioI in various bound states were also determined by assessment of its effects on the secondary structure using far-UV CD spectroscopy. By measuring the proportional change in ellipticity at 219 nm between BioI samples in 0 M GdmCl (fully folded) and 7 M GdmCl (fully unfolded), it was found that there were minimal effects of the binding of various ligands and substrates on the GdmCl concentration required to induce loss of 50% of the secondary structure. Plots of percent loss of ellipticity at 219 nm versus GdmCl concentration described sigmoids and were fitted to eq 2 to yield a midpoint K^U value that was consistently in the range 1.84 ± 0.23 M GdmCl regardless of the ligand or substrate. Thus, it appears that there are negligible effects on stability of secondary structure of BioI induced by substrate or ligand binding to the enzyme.

EPR analysis of BioI at pH 7.5 in the form isolated from the *E. coli* expression host indicates a heterogeneous population of high-spin/low-spin (HS/LS) heme, as observed also by UV−visible absorption spectroscopy (Figure 7, panel B). A rhombic trio was observed with *g*-values at $g = 2.42$ (g_z),

2.25 (g_y), and 1.92 (g_x), reflecting a typical low-spin P450 heme. The values are close to those reported previously for the well-characterized P450 BM3 heme domain (2.41, 2.25, 1.91) (*12*) and to those previously reported for BioI (2.41, 2.24, 1.97/1.91) (*16*). In the previous study by Green et al., some heterogeneity in the low-spin g_x value was observed with signals at both $g = 1.97$ and 1.91 (16). Here, we are able to better resolve this heterogeneity, distinguishing two distinct low-spin forms of BioI at pH 7.5. The second species has its *g*-values at 2.47, 2.25, and 1.98. Carbon monoxide-binding studies show that the BioI preparation used was essentially all P450. Thus, presence of an inactive P420 component as an explanation for the heterogeneity of the low-spin form can be ruled out. A triplet of signals typical of a considerable proportion of high-spin BioI is also present at pH 7.5 (8.14, 3.48, 1.67). Again, the high-spin signals are consistent with those reported previously for the camphor hydroxylase P450 cam and other P450s (*48*). EPR spectroscopy of the same enzyme preparation at pH 9.5 (Figure 7, panel A) shows the virtually complete removal of the high-spin component, as suggested from optical studies. In addition, the heterogeneity of the low-spin species is dramatically decreased with the more "typical" rhombic trio at 2.42, 2.25, and 1.92 predominating. On addition of testosterone at pH 7.5, the high-spin component is also effectively removed with the major signal being the "typical" low-spin triplet at 2.42, 2.25, 1.92 (Figure 7, panel C). This may suggest that the effect of the testosterone is to reinforce a native-like aqua-cys ligated ferric heme iron, as opposed to coordinating directly itself to the iron via a carbonyl group. However, at this stage we cannot rule out the possibility that the EPR signals for the two different types of oxygen coordination at the distal position can give rise to highly similar EPR spectra. Also in the testosterone-bound form, another minor species is evident with a low-spin triplet at 2.54, 2.25, 1.89. Potentially, this might reflect a proportion of the enzyme in a steroid carbonyl-ligated form. However, previous EPR studies of human endothelial nitric oxide synthase (eNOS) and *Fusarium oxysporum* P450 nor have revealed similar triplets of *g*-values, considered to reflect minor populations of another low-spin ligand-free cys-aqua ligated ferric heme species (*49*, *50*). Thus, it is also feasible that these EPR data for the testosterone-ligated BioI reveal the presence of two distinct cys-aqua ligated species. Regardless of whether carbonyl ligation to the BioI iron occurs in the testosterone-bound enzyme, it is clear that this (and similar steroids) bind tightly and induce a near-complete conversion to a low-spin ferric heme iron species.

Resonance Raman spectra were collected for BioI as purified from *E. coli*, for the testosterone-bound, fatty acid-bound (palmitoleic acid, myristoleic acid), and econazole-bound forms (at pH 7.0), and for BioI as purified from *E. coli* at pH 9.5. The spectra recorded were highly similar to those reported previously with the dominant $\nu 4$ signal at 1372 cm^{-1} indicating the presence of only ferric heme iron in the samples (*16*). However, spectral analysis of the various forms of BioI indicate clear differences in the degree of "splitting" of the spin-state-sensitive $\nu 3$ band. Heterogeneity of the $\nu 3$ signal was observed previously in the study of palmitate-bound BioI purified from *E. coli* and is consistent with a mixture of high- and low-spin forms of the enzyme (*16*). The $\nu 3$ features in BioI are located at 1501 and 1487 cm^{-1} with the higher wavenumber feature indicative of the low-spin component and the lower one indicative of the high-spin component. For the testosterone-bound, econazole-bound, and pH 9.5 samples, the magnitude of the feature at 1501 cm^{-1} is much larger than that at 1487 cm^{-1}, indicating predominance of the low-spin form. For the fatty acid-bound forms, the 1487 cm^{-1} form is more intense, as expected for a high-spin enzyme. The BioI form purified from *E. coli*, with palmitate bound in a proportion of molecules, has an intermediate spectrum with both $\nu 3$ features being of similar intensity, indicating a similar proportion of the two forms, in agreement with the optical data.

Potentiometric Studies. Potentiometric studies were performed on BioI in a variety of ligand-bound and ligand-free forms, as described in the Experimental Procedures section. BioI purified from *E. coli* was consistently found to be in a mixed spin-state form, that is, with considerable proportions of both low- and high-spin forms of the heme iron. At 25 °C (the temperature at which the redox titrations are performed), the A_{390} (absorption wavelength typical of the high-spin form) was invariably of very similar intensity to the A_{419} (typical of the low-spin form), suggesting roughly equal proportions of the two forms. As discussed above, this behavior results from copurification of BioI with a lipid substrate from *E. coli* (palmitate), rather than being due to a natural "poise" of the high-spin and low-spin forms in a close equilibrium due to the electronic properties of the system. Potentiometric titration of a palmitate-bound BioI sample as purified from *E. coli* yielded a midpoint reduction potential of -228 ± 4 mV. The redox titration was completely reversible in reductive and oxidative directions, without development of turbidity due to enzyme aggregation and with no sign of hysteretical behavior (i.e., the spectra collected at similar potentials during oxidative and reductive titrations were essentially identical, Figure 8). The reduced form of the enzyme had its Soret band shifted to ~406 nm with apparent spectral fusion of the α and β bands with maximum at ~552 nm.

Since this sample of P450 BioI was effectively a partially substrate (palmitate)-bound enzyme, further potentiometric studies were performed with enzymes saturated with the tight-binding fatty acid palmitoleic acid (i.e., as near complete high-spin form as possible) and following addition of testosterone and at pH 9.0 (i.e., as near complete low-spin heme iron as possible). Treatment of another sample from the same preparation with 15% (v/v) ethanol, followed by gel filtration to remove the solvent, produced a low-spin form that underwent complete conversion to a nativelike spectral form on addition of dithionite reductant and introduction of carbon monoxide (i.e., the P450 form with Soret absorption maximum at 448 nm). Potentiometric study of the resultant low-spin form of BioI showed that the enzyme could be reversibly reduced and reoxidized as normal without hysteretic behavior or protein aggregation but that the midpoint potential was now more negative at -330 ± 5 mV. Otherwise, the spectral features of the reduced form were indistinguishable from those observed previously. Elevation of the pH to 9.5 also induced complete conversion to the low-spin form, and redox titration at this pH produced a virtually identical E_1' value for the heme Fe^{3+}/Fe^{2+} transition of -330 ± 3 mV. Also, as shown above, addition of steroids promotes conversion of the enzyme to a species with spectral

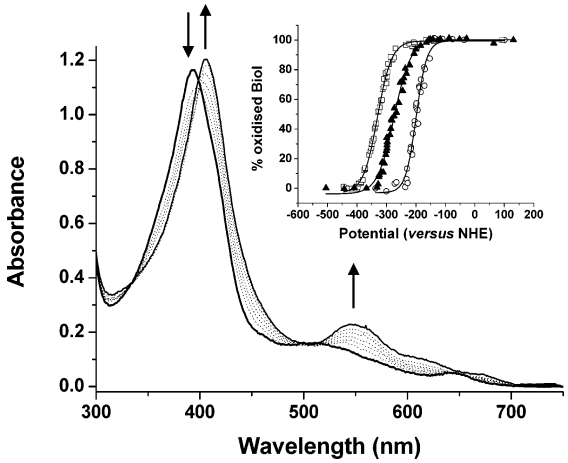

FIGURE 8: Redox titrations of BioI in different forms. The main figure shows the spectral changes accompanying the conversion of palmitoleic acid-bound P450 BioI (~12.5 μM) from its oxidized (ferric) form (thick, solid line) with Soret maximum at ~394 nm to its reduced (ferrous) form (thin, solid line) with Soret maximum at ~406 nm. Selected spectra recorded at intermediate points in the titration are shown as dotted lines. Arrows indicate direction of absorption change for the major absorption bands as the titration progresses in the reductive direction. The inset shows an overlay of redox titration data (absorption change reflecting proportion of heme oxidized versus reduction potential, reported with reference to the normal hydrogen electrode, NHE) for the palmitoleic acid-bound form of P450 BioI (○), the testosterone-bound form (▲), and the partially palmitate-bound form isolated from *E. coli* at pH 9.5 (□). Data are fitted to the Nernst equation (eq 3) yielding midpoint reduction potentials of 199 ± 3, −273 ± 4, and −330 ± 3 mV, respectively. Spectra were collected and data processed as described in the Experimental Procedures section.

properties typical of the low-spin form of BioI. A redox titration was also performed for BioI in the testosterone-bound form. In this case, the Soret band for the steroid-bound form was located at 419 nm in the oxidized state and moved to ~407 nm in the reduced (ferrous) species; a similar spectral shift to that observed for the reduction of the enzyme at pH 9.5. However, the potential for the transition (−273 ± 4 mV) was rather more positive than that observed for BioI incubated at pH 9.5 or pretreated with ethanol to induce conversion to a low-spin form.

A more positive heme iron reduction potential is expected on conversion of the heme iron to the high-spin form, as observed for potentiometric measurements in the P450cam and P450 BM3 systems (*40*, *51*). Saturation with the fatty acid substrate palmitoleic acid converted BioI almost completely to the high-spin form. Redox titration of this species produced a midpoint potential of −199 ± 3 mV, more positive than that for low-spin forms generated either by solvent extraction, by high pH, or by testosterone binding by approximately 131, 131, and 74 mV, respectively. The 131 mV shift observed between the low-spin ligand-free form and the substrate-saturated form is consistent with the extent of potential shift observed previously for P450 BM3 and P450 cam (*40*, *51*).

DISCUSSION

Recent genome sequencing efforts have led to the understanding that P450 enzymes are widespread in bacteria and that many are likely to have roles in biosynthetic processes. Perhaps most notable is the preponderance of CYP genes in the actinomycete bacteria, where P450s are implicated in synthesis of polyketide molecules. However, the bacilli also possess a number of P450 enzymes. The genome sequence of the 168 strain of *B. subtilis* indicates seven distinct P450s, and of these, at least P450 BioI has a biosynthetic role in the manufacture of the vitamin biotin (*17*). In the related W23 strain, a further P450 of unknown function (CYP109A1) is present. To date, BioI is the only P450 proposed to have a role in vitamin biosynthesis. Perhaps the best characterized of the biosynthetic bacterial P450s is P450 eryF (CYP107A1) from *S. erythraea*, which catalyzes the final step in the synthesis of the polyketide antibiotic erythromycin (*29*). P450 eryF displays considerable amino acid sequence similarity to P450 BioI (34.4% identity), perhaps suggesting common structural features that extend beyond the basic "core" P450 structure. Certainly from this study, BioI has in common with P450 eryF the capacity to bind both steroids and polycyclic azole drugs. However, the physiological substrates of BioI are considered to be long-chain fatty acids or their CoA esters (*16*, *18*). Thus, the flexibility of the active site of BioI is obvious from its ability to bind both long-chain fatty acids and polycyclic molecules. Azole drugs and selected steroids tested have tighter binding constants than many of the fatty acids that bind BioI, presumably mainly due to favorable interactions with the heme iron, as well as with active site residues. Only steroids with a carbonyl group at the C_3 position produced spectral perturbations in BioI; those with a hydroxyl group at the same carbon did not. While the spectral perturbation produced by steroids such as testosterone indicated conversion to a species that resembles an aqua-cys ligated low-spin P450 heme (Soret maximum at 418 nm), modeling suggests that the reason for the apparent discrimination between the C_3−OH and C_3═O steroids is that the carbonyl group in the latter class of molecules may interact directly with the heme iron. In the testosterone-bound form of BioI, EPR indicates that the heme is converted to an almost completely low-spin form (from the mixed-spin, partially palmitate-bound form isolated from *E. coli*) but that the predominant species present has EPR properties indistinguishable from that of the cys-aqua ligated ferric form of BioI. Thus, we cannot at this point be certain that the spectral effects induced by binding of the C_3═O-containing steroids is mediated by direct ligation to the heme iron. However, what is clear is that the reduction potential of the heme iron in the testosterone-bound form of BioI is ~60 mV more positive than that of the low-spin forms of the enzyme generated by solvent treatment or by incubation at pH 9.5. Possibly, this arises due to the direct influence on the heme or its distal aqua ligand mediated by the steroid. However, an alternative explanation would be that there is direct interaction between the steroid carbonyl and the ferric heme iron. Among the steroids that were found to induce spectral perturbation on binding to P450 BioI, it was apparent that (compared with testosterone) the presence of substituents on the C ring reduced binding affinity (probably due to steric clash) while substituents on the D ring affected K_d values to a much lesser extent.

Attempts to date to isolate diffracting crystals of BioI have not been successful. However, our recent studies have shown promise in terms of isolating crystals of BioI in complex with host glyceraldehyde 3-phosphate dehydrogenase (GAPDH), with which it copurifies from *E. coli* (Lawson, R. J. et

al., manuscript in preparation). To gain information on the structural organization of P450 BioI in advance of a true structure from X-ray crystallography, we built a model of BioI based on the structures of other bacterial enzymes. The model indicates that a disulfide bond is present in the oxidized enzyme between cysteines 250 and 275. Alignment of the amino acid sequence of BioI with several hundred of the other available P450 amino acid sequences in the database suggested that this arrangement of cysteines is unique in P450s sequenced to date and that a disulfide formed in such a way in a P450 may be virtually exclusive to P450 BioI. This finding is in accord with the improved expression of BioI in a *gor*, *trx* mutant strain of *E. coli*, but structural stability studies indicate that reduction of the disulfide with dithiothreitol has rather minor effects on BioI. The position of the disulfide (approximately 11 Å from the closest contact to the heme macrocycle) means that a potential role in electron transfer to the heme cannot be ruled out. This aspect is currently under investigation, but at present, we have no evidence to suggest that the disulfide plays anything other than a structural role. Nonetheless, this is the first evidence for a disulfide bond in a P450 enzyme. Despite an apparent lack of change in T_m value in the presence of the disulfide reductant DTT, DSC studies do indicate a destabilization of BioI (lower T_m) in the presence of fatty acid, perhaps suggesting a structural change induced on fatty acid binding similar to that observed for P450 BM3 (*45*).

Molecular modeling of the interaction of BioI with a fatty acid substrate (myristic acid) indicates that positioning of the ω-carbon of the substrate is close to the heme iron and that any oxygenation reactions should occur close to this end of the fatty acid. This is in agreement with previous work by Green et al. (*16*) and is further confirmed by the turnover studies reported in the accompanying manuscript, where *B. subtilis* flavodoxins are used to drive BioI catalysis. These data appear to contrast with the earlier paper of Stok and De Voss, who reported that BioI could catalyze carbon−carbon bond cleavage at the central carbons of lipid substrates to generate small amounts of the C_7 dicarboxylic acid pimelic acid (*18*). In our model, steric restrictions prevent the orientation of a fatty acid substrate appropriate for oxidative attack at its central carbons (specifically, at ω-7 for myristic acid). In more recent work, De Voss and colleagues demonstrated that (in single turnover conditions with large excess of BioI over substrate) BioI catalyzed hydroxylation of fatty acids close to the ω-terminal with myristic acid being hydroxylated at the ω-1, ω-2, and ω-3 positions (*46*). This is in agreement with study of Green et al. (*16*) and with the data reported in the accompanying paper. Thus, capacity to perform a series of reactions at the central carbon(s) of a long-chain fatty acid molecule to produce (ultimately) pimelic acid appears unfavorable in this particular type of redox system. It has been suggested that the adventitious binding of *E. coli* acyl carrier protein (ACP) to BioI mimics the binding of a homologous ACP in the *Bacillus* species, enabling production of pimelic acid (*18*). However, molecular modeling predicts that a large conformational readjustment of BioI would be required to facilitate oxidative attack of myristic acid at the correct position. Further evidence in favor of the capacity of BioI to catalyze this bond cleavage reaction was presented very recently (*52*). Thus, if the proposed carbon−carbon bond cleavage reaction is the physiologically relevant one, our modeling studies suggest that docking of ACP must induce a large structural perturbation in the P450 to facilitate correct orientation of the lipid in its active site. In this study (as previously, *16*), we did not coisolate ACP protein with BioI from our expression system. As indicated above, however, substoichiometric amounts of *E. coli* GAPDH were coisolated with BioI.

Potentiometric studies have provided the first description of the reduction potentials of the P450 BioI heme iron in different forms. Thermodynamically, BioI exhibits behavior typical of the soluble bacterial P450s characterized to date with an elevation of ~130 mV in heme iron reduction potential between the substrate-free low-spin form and the fatty acid-bound high-spin form. It is likely that, as with the P450 BM3 and P450 cam systems, substrate binding leads to displacement of a weakly bound aqua ligand at the distal coordination position on the heme iron and produces a change in heme iron spin-state equilibrium in favor of the high-spin form. The high-spin form can then be more easily reduced by the physiological redox partner, so triggering (or accelerating) electron transfer and productive catalysis. In the accompanying paper, we investigate electron transfer from and interactions with the flavodoxins from *B. subtilis* (YkuN and YkuP) and demonstrate that they can support BioI catalysis.

Detailed EPR studies of BioI reveal spectral heterogeneity in the low-spin form of BioI, which is not associated with the presence of any P420 form of the enzyme. An explanation for the presence of a second low-spin form of BioI is that bound lipid (i.e., palmitate from the expression host) interacts with the heme or heme iron in a proportion of BioI in the low-spin (cys-aqua ligated) form. The fact that both incubation at pH 9.5 and addition of testosterone result in the loss of the second low-spin species (in favor of the "typical" P450 low-spin signal) suggests that this is a likely scenario, since both treatments should result in displacement of fatty acids from the proximity of the heme iron. As expected, both treatments effectively remove completely the high-spin form of BioI, for which we also provide the first EPR characterization here.

In conclusion, we report here a detailed thermodynamic and spectroscopic characterization of P450 BioI. Our data demonstrate unexpected flexibility of the active site with the capacity to bind tightly to certain steroids and to bulky azole drugs, as well as long-chain fatty acids. It is also demonstrated that BioI is purified from *E. coli* with palmitic acid bound. This explains its isolation in a mixed spin state. Alteration of pH or brief treatment with small amounts of an appropriate solvent releases the lipid and converts the P450 to a low-spin form. Potentiometric studies show that there is an ~130 mV difference in the reduction potentials of the low-spin and high-spin forms of the enzyme, and this shift in spin state and potential of the heme iron as substrate binds likely occurs on binding of lipid substrate in vivo and precedes electron transfer from redox partners. Modeling studies predict the presence of a disulfide bond in BioI, and this was validated by free cysteine thiol measurements in the presence and absence of dithiothreitol. This is the first report of a disulfide bond in a cytochrome P450 enzyme. In ongoing studies, we are investgating the effects of mutations to the cysteines involved in the predicted BioI disulfide on expression, stability, and biophysical properties of the P450.

ACKNOWLEDGMENT

A.W.M. thanks the Royal Society for the award of a Leverhulme Trust Senior Research Fellowship. The authors are also grateful to Professor Andrew Thomson at the University of East Anglia, Centre for Metalloprotein Spectroscopy and Biology, for access to facilities and helpful discussions.

REFERENCES

1. Munro, A. W., and Lindsay, J. G. (1996) Bacterial cytochromes P450, *Mol. Microbiol. 20*, 1115−1125.
2. Guengerich, F. P. (1991) Reactions and significance of cytochrome P-450 enzymes, *J. Biol. Chem. 266*, 10019−10022.
3. Guengerich, F. P. (1995) Human cytochrome P450 enzymes, in *Cytochrome P450 Structure, Mechanism and Biochemistry*. (Oriz de Montellano, P. R., Ed.) pp 537−574, Plenum Press, New York.
4. Williams, P. A., Cosme, J., Sridhar, V., Johnson, E. F., and McRee, D. E. (2000) Mammalian microsomal cytochrome P450 monooxygenase: Structural adaptations for membrane binding and functional diversity, *Mol. Cell 5*, 121−131.
5. Leys, D., Mowat, C. G., McLean, K. J., Richmond, A., Chapman, S. K., Walkinshaw, M. D., and Munro, A. W. (2003) Atomic structure of *Mycobacterium tuberculosis* CYP121 to 1.06 Å reveals novel features of cytochrome P450, *J. Biol. Chem. 278*, 5141−5147.
6. Poulos, T. L., Finzel, B. C., and Howard, A. J. (1986) Crystal structure of substrate-free *Pseudomonas putida* cytochrome P-450cam, *Biochemistry 25*, 5314−5322.
7. Hasemann, C. A., Ravichandran, K. G., Peterson, J. A., and Deisenhofer, J. (1994) Crystal structure and refinement of cytochrome $P450_{terp}$ at 2.3 Angstrom resolution, *J. Mol. Biol. 236*, 1169−1185.
8. Cupp-Vickery, J. R., and Poulos, T. L. (1995) Structure of cytochrome P450eryF involved in erythromycin biosynthesis, *Nat. Struct. Biol. 2*, 144−153.
9. Kunst, K., Ogasawara, N., Moszer, I., Albertini, A. M., Azevedo, V., et al. (1997) The complete genome sequence of the Gram-positive bacterium *Bacillus subtilis*, *Nature 390*, 249−256.
10. Narhi, L. O., and Fulco, A. J. (1987) Identification and characterization of 2 functional domains in cytochrome P-450 BM3: A catalytically self-sufficient mono-oxygenase induced by barbiturates in *Bacillus megaterium*, *J. Biol. Chem. 262*, 6683−6690.
11. Munro, A. W., Leys, D. G., McLean, K. J., Marshall, K. R., Ost, T. W. B., Daff, S., Miles, C. S., Chapman, S. K., Lysek, D. A., Moser, C. C., Page, C. C., and Dutton, P. L. (2002) P450 BM3: The very model of a modern flavocytochrome, *Trends Biochem. Sci. 27*, 250−257.
12. Miles, J. S., Munro, A. W., Rospendowski, B. N., Smith, W. E., McKnight, J., and Thomson, A. J. (1992) Domains of the catalytically self-sufficient cytochrome P-450 BM-3: Genetic construction, overexpression, purification and spectroscopic characterization, *Biochem. J. 288*, 503−509.
13. Gustafsson, M. C. U., Roitel, O., Marshall, K. R., Noble, M. A., Chapman, S. K., Pessegueiro, A., Fulco, A. J., Cheesman, M. R., von Wachenfeldt, C., and Munro, A. W. Expression, purification and characterization of *Bacillus subtilis* cytochromes P450 CYP102A2 and CYP102A3. Flavocytochrome homologues of P450 BM3 from *Bacillus megaterium*, *Biochemistry*, in press.
14. Lee, D. S., Yamada, A., Sugimoto, H., Matsunaga, I., Ogura, H., Ichihara, K., Adachi, S., Park, S. Y., and Shiro, Y. (2003) Substrate recognition and molecular mechanism of fatty acid hydroxylation by cytochrome P450 from *Bacillus subtilis* − Crystallographic, spectroscopic, and mutational studies, *J. Biol. Chem. 278*, 9761−9767.
15. Matsunaga, I., Yamada, A., Lee, D. S., Obayashi, E., Fujiwara, N., Kobayashi, K., Ogura, H., and Shiro, Y. (2002) Enzymatic reaction of hydrogen peroxide-dependent peroxygenase cytochrome P450s: Kinetic deuterium isotope effects and analyses by resonance Raman spectroscopy, *Biochemistry 41*, 1886−1892.
16. Green, A. J., Rivers, S. L., Cheesman, M., Reid, G. A., Quaroni, L. G., Macdonald, I. D. G., Chapman, S. K., and Munro, A. W. (2001) Expression, purification and characterization of cytochrome P450 BioI: a novel P450 involved in biotin synthesis in *Bacillus subtilis*, *J. Biol. Inorg. Chem. 6*, 523−533.
17. Bower, S., Perkins, J. B., Yocum, R. R., Howitt, C. L., Rahaim, P., and Pero, J. (1996) Cloning, sequencing, and characterization of the *Bacillus subtilis* biotin biosynthetic operon, *J. Bacteriol. 178*, 4122−4130.
18. Stok, J. E., and De Voss, J. J. (2000) Expression, purification, and characterization of bioI: A carbon−carbon bond cleaving cytochrome P450 involved in biotin biosynthesis in *Bacillus subtilis*, *Arch. Biochem. Biophys. 384*, 351−360.
19. Tosha, T., Yoshioka, S., Hori, H., Takahashi, S., Ishimori, K., and Morishima, I. (2002) Molecular mechanism of the electron-transfer reaction in cytochrome $P450_{cam}$-putidaredoxin: Roles of glutamine 360 at the heme proximal site, *Biochemistry 41*, 13883−13893.
20. Muller, J. J., Lapko, A., Bourenkov, G., Ruckpaul, K., and Heinemann, U. (2001) Adrenodoxin reductase-adrenodoxin complex structure suggests electron-transfer path in steroid biosynthesis, *J. Biol. Chem. 276*, 2786−2789.
21. Green, A. J., Munro, A. W., Cheesman, M. R., Reid, G. A., von Wachenfeldt, C., and Chapman, S. K. (2003) Expression, purification and characterisation of a *Bacillus subtilis* ferredoxin: a potential electron transfer donor to cytochrome P450 BioI, *J. Inorg. Biochem. 93*, 92−99.
22. Sambrook, J., Fritsch, E. F., and Maniatis, T. (1989) *Molecular Cloning, a laboratory manual*, 2nd ed., Cold Spring Harbor Laboratory Press, Cold Spring Harbor, NY.
23. Omura, T., and Sato, R. (1962) A new cytochrome in liver microsomes, *J. Biol. Chem. 237*, 1375−1376.
24. Murataliev, M. B., and Feyereisen, R. (2000) Functional interactions in cytochrome $P450_{BM3}$. Evidence that NADP(H) binding controls redox potentials of the flavin cofactors, *Biochemistry 39*, 12699−12707.
25. Berman, H. M., Westbrook, J., Feng, Z., Gilliland, G., Bhat, T. N., Weissig, H., Shindyalov, I. N., and Bourne, P. E. (2000) The protein data bank, *Nucleic Acids Res. 28*, 235−242.
26. Altschul, S. F., Madden, T. L., Schaffer, A. A., Zhang, J., Zhang, Z., Miller, W., and Lipman, D. J. (1997) Gapped BLAST and PSI-BLAST: a new generation of protein database search programs, *Nucleic Acids Res. 25*, 3389−3402.
27. Hasemann, C. A., Ravichandran, K. G., Peterson, J. A., and Deisenhofer, J. (1994) Crystal structure and refinement of cytochrome P450terp at 2.3 Å resolution, *J. Mol. Biol. 236*, 1169−1185.
28. Ravichandran, K. G., Boddupalli, S. S., Hasermann, C. A., Peterson, J. A., and Deisenhofer, J. (1993) Crystal structure of hemoprotein domain of P450 BM-3, a prototype for microsomal P450's, *Science 261*, 731−736.
29. Cupp-Vickery, J. R., and Poulos, T. L. (1995) Structure of cytochrome P450eryF involved in erythromycin biosynthesis, *Nat. Struct. Biol. 2*, 144−153.
30. Sali, A., and Blundell, T. L. (1993) Comparative protein modelling by satisfaction of spatial restraints, *J. Mol. Biol. 234*, 779−815.
31. Thompson, J. D., Higgins, D. G., and Gibson, T. J. (1994) CLUSTAL W: improving the sensitivity of progressive multiple sequence alignment through sequence weighting, position-specific gap penalties and weight matrix choice, *Nucleic Acids Res. 22*, 4673−4680.
32. Lewis, D. F. V. (1986) Physical methods in the study of the active site geometry of cytochromes P-450, *Drug Met. Rev. 17*, 1−66.
33. Kabsch, W., and Sander, C. (1983) Dictionary of protein secondary structure: pattern recognition of hydrogen-bonded and geometrical features, *Biopolymers 22*, 2577−2637.
34. Jones, D. T. (1999) Protein secondary structure prediction based on position-specific scoring matrices, *J. Mol. Biol. 292*, 195−202.
35. Kelley, L. A., Gardner, S. P., and Sutcliffe, M. J. (1996) An automated approach for clustering an ensemble of NMR-derived protein structures into conformationally related subfamilies, *Protein Eng. 9*, 1063−1065.
36. Jones, B. C., Tyman, C. A., and Smith, D. A. (1997) Identification of the cytochrome P450 isoforms involved in the O-demethylation of 4-nitroanisole in human liver microsomes, *Xenobiotica 27*, 1025−1037.
37. Riddles, P. W., Blakeley, R. L., and Zerner, B. (1983) Reassessment of Ellman's reagent, *Methods Enzymol. 91*, 49−60.
38. Munro, A. W., Noble, M. A., Robledo, L., Daff, S., and Chapman, S. K. (2001) Determination of the redox properties of human NADPH-cytochrome P450 reductase, *Biochemistry 40*, 1956−1963.

39. Daff, S. N., Chapman, S. K., Turner, K. L., Holt, R. A., Govindaraj, S., Poulos, T. L., and Munro, A. W. (1997) Redox control of the catalytic cycle of flavocytochrome P450 BM3, *Biochemistry 36*, 13816−13823.
40. Dutton, P. L. (1978) Redox potentiometry: Determination of midpoint potentials of oxidation−reduction components of biological electron-transfer systems, *Methods Enzymol. 54*, 411−435.
41. Noble, M. A., Miles, C. S., Chapman, S. K., Lysek, D. A., MacKay, A. C., Reid, G. A., Hanzlik, R. P., and Munro, A. W. (1999), Roles of key active-site residues in flavocytochrome P450 BM3, *Biochem. J. 339*, 371−379.
42. Kobayashi, K., Ehrlich, S. D., Albertini, A., Amati, G., Andersen, K. K., et al. Essential *Bacillus subtilis* genes, *Proc. Natl. Acad. Sci. U.S.A. 100*, 4678−4683.
43. Lee, D. S., Yamada, A., Sugimoto, H., Matsunaga, I., Ogura, H., Ichihara, K., Adachi, S., Park, S. Y., and Shiro, Y. (2003) Substrate recognition and molecular mechanism of fatty acid hydroxylation by cytochrome P450 from *Bacillus subtilis* − crystallographic, spectroscopic and mutational studies, *J. Biol. Chem. 278*, 9761−9767.
44. Cupp-Vickery, J., Anderson, R., and Hatziris, Z. (2000) Crystal structures of ligand complexes of P450eryF exhibiting homotropic cooperativity, *Proc. Natl. Acad. Sci. U.S.A. 97*, 3050−3055.
45. Li, H. Y., and Poulos, T. L. (1997) The structure of the cytochrome P450 BM-3 haem domain complexed with the fatty acid substrate, palmitoleic acid, *Nat. Struct. Biol. 4*, 140−146.
46. Cryle, M. J., Matovic, N. J., and De Voss, J. J. (2003) Products of cytochrome $P450_{BioI}$ (CYP107H1)-catalyzed oxidation of fatty acids, *Org. Lett. 5*, 3341−3344.
47. Munro, A. W., Lindsay, J. G., Coggins, J. R., Kelly, S. M., and Price, N. C. (1996) Analysis of the structural stability of the multidomain enzyme flavocytochrome P-450 BM3, *Biochim. Biophys. Acta 1296*, 127−137.
48. Lewis, D. F. V. (1996) *Cytochromes P450: Structure, Function and Mechanism*, Taylor and Francis, London.
49. Berka, V., Palmer, G., Chen, P. F., and Tsai, A. L. (1998) Effects of various imidazole ligands on heme conformation in endothelial nitric oxide synthase, *Biochemistry 37*, 6136−6144.
50. Shiro, Y., Fujii, M., Isogai, Y., Adachi, S., Izuka, T., Obayashi, E., Makino, R., Nakahara, K., and Shoun, H. (1995) Iron-ligand structure and iron redox property of nitric oxide reductase cytochrome P450nor from *Fusarium oxysporum*: Relevance to its NO reduction activity, *Biochemistry 34*, 9052−9058.
51. Sligar S. G. (1976) Coupling of spin, substrate, and redox equilibria in cytochrome P450, *Biochemistry 15*, 5399−5406.
52. Cryle, M. J., and De Voss, J. J. (2004) Carbon−carbon bond cleavage by cytochrome $P450_{BioI}$ (CYP107H1), *Chem. Commun.*, 86−87.
53. Lu, P., Alterman, M. A., Chaurasia, C. S., Bambal, R. B., and Hanzlik, R. P. (1997) Heme-coordinating analogues of lauric acid as inhibitors of fatty acid omega-hydroxylation, *Arch. Biochem. Biophys. 337*, 1−7.
54. Belitsky, B. R., Gustafsson, M. C., Sonenshein, A. L., and Von Wachenfeldt, C. (1997) An lrp-like gene of *Bacillus subtilis* involved in branched-chain amino acid transport, *J. Bacteriol. 179*, 5448−5457.

BI049132L